Using fluorescence and bioluminescence sensors to characterize auto- and heterotrophic plankton communities

Monique Messié, Igor Shulman, Severine Martini, Steven H.D. Haddock

Progress in Oceanography 171 (2019) 76–92

Contents lists available at ScienceDirect

Progress in Oceanography

journal homepage: www.elsevier.com/locate/pocean

Using fluorescence and bioluminescence sensors to characterize auto- and heterotrophic plankton communities

Monique Messié[a,b,*], Igor Shulman[c], Séverine Martini[d], Steven H.D. Haddock[a]

[a] Monterey Bay Aquarium Research Institute, Moss Landing, CA 95039, USA
[b] Aix Marseille Univ., Université de Toulon, CNRS, IRD, MIO UM 110, 13288 Marseille, France
[c] US Naval Research Laboratory, Stennis Space Center, MS 39529, USA
[d] Sorbonne Université, CNRS, Laboratoire d'Océanographie de Villefranche, LOV, F-06230 Villefranche-sur-mer, France

ARTICLE INFO

Keywords:
Bioluminescence
Fluorescence
Phytoplankton
Zooplankton
Coastal upwelling
Time series

ABSTRACT

High-resolution autonomous sensors routinely measure physical (temperature, salinity), chemical (oxygen, nutrients) and biological (fluorescence) parameters. However, while fluorescence provides a proxy for phytoplankton, heterotrophic populations remain challenging to monitor in real-time and at high resolution. Bathyphotometers, sensors which measure the light emitted by bioluminescent organisms when mechanically stimulated, provide the capability to identify bioluminescent dinoflagellates and zooplankton. In the coastal ocean, highly abundant dinoflagellates emitting low-intensity flashes generate a background bioluminescence signal, while rarer zooplankton emit bright flashes that can be individually resolved by high-frequency sensors. Bathyphotometers were deployed from ships and onboard autonomous underwater vehicles (AUVs) during three field campaigns in Monterey Bay, California. Ship-based *in situ* water samples were simultaneously collected and the plankton communities characterized. Plankton concentrations were matched with concurrent datasets of fluorescence and bioluminescence to develop proxies for autotrophic and heterotrophic dinoflagellates, other phytoplankton such as diatoms, copepods, larvaceans (appendicularians), and small jellies. The method extracts the bioluminescence background as a proxy for dinoflagellates, and exploits differences in bioluminescence flash intensity between several types of zooplankton to identify larvaceans, copepods and small jellies. Fluorescence is used to discriminate between autotrophic and heterotrophic dinoflagellates, and to identify other autotrophic plankton. Concurrent fluorometers and bathyphotometers onboard AUVs can thus provide a novel view of plankton diversity and phytoplankton/zooplankton interactions in the sea.

1. Introduction

Autonomous platforms such as profiling floats, gliders or autonomous underwater vehicles (AUVs) have revolutionized oceanography by providing high-resolution, continuous measurements across the water column. In the field of biological oceanography, the early integration of fluorometers onboard autonomous platforms have provided unprecedented views of phytoplankton structure and variability in the upper ocean (e.g., Mahadevan et al., 2012; Rudnick, 2016). Other biological sensors have been integrated into gliders and AUVs in recent years, targeting zooplankton, fish, and larger animals using acoustic backscatter (Powell and Ohman, 2012) and echo sounders (Moline et al., 2015). Despite these advances, the characterization of biological communities remains elusive, particularly for small plankton. Most optical and acoustic sensors only measure bulk properties and cannot distinguish between taxonomic groups, although ratios of fluorescence to optical backscatter have been shown to correlate with phytoplankton community composition (Cetinić et al., 2015). Recent advances using spectral fluorescence show promise in characterizing phytoplankton community composition (Richardson et al., 2010) but have not yet been integrated onboard autonomous platforms to our knowledge. Imaging and ecogenomic sensors targeting phytoplankton and zooplankton provide taxonomic information but come with their own set of challenges, such as power requirements, size, data telemetry, environment, and cost (Lopez et al., 2015).

In the family of biological autonomous sensors, bathyphotometers (sensors which measure the light emitted by small bioluminescent organisms when mechanically stimulated) are at the intersection between "bulk" and "taxon-specific" sensors. Bioluminescence as measured by a bathyphotometer is a bulk property that scales with biomass for a given planktonic community (Lapota, 1998; Latz and Rohr, 2013). In addition, characteristics of bioluminescent emissions such as flash shape,

* Corresponding author.
E-mail address: monique@mbari.org (M. Messié).

https://doi.org/10.1016/j.pocean.2018.12.010
Received 23 February 2018; Received in revised form 12 December 2018; Accepted 13 December 2018
Available online 14 December 2018

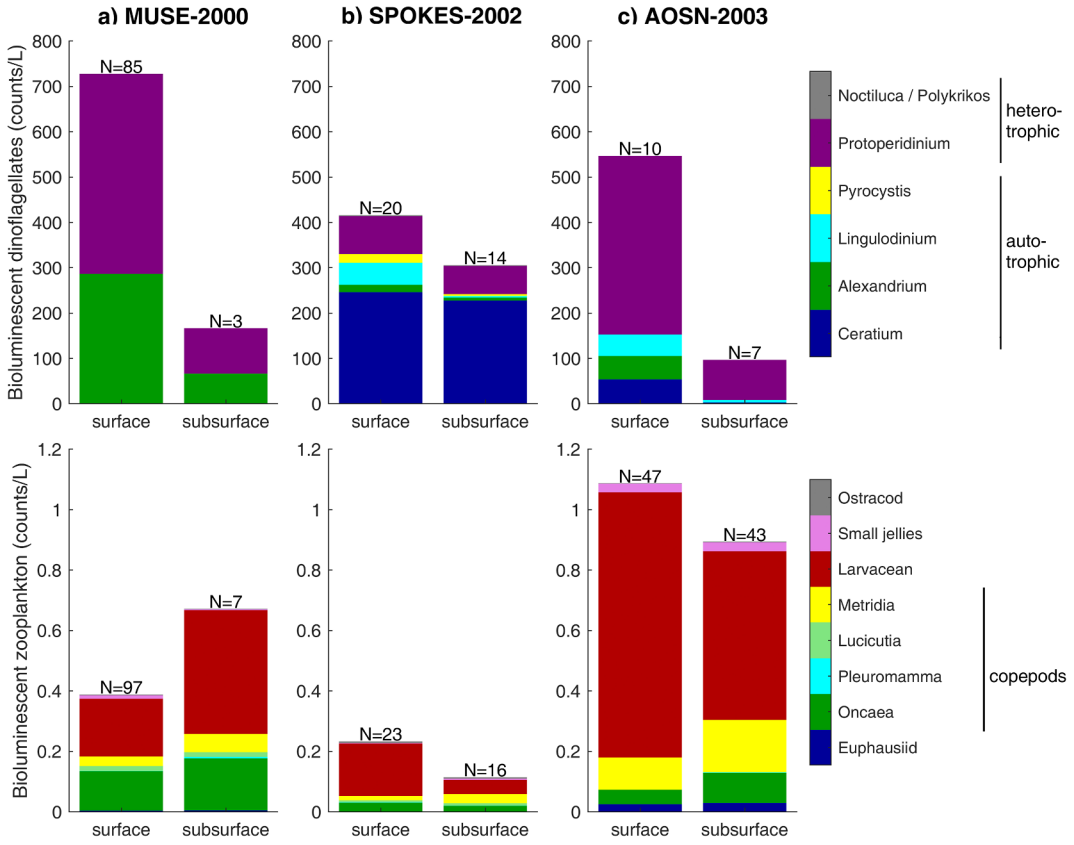

Fig. 1. Average bioluminescent plankton community composition measured during three field campaigns in Monterey Bay, California (top: phytoplankton, bottom: zooplankton). Field campaigns and sampling are described in Section 2.5. Samples are separated between surface (shallower than 20 m) and subsurface (below 20 m). The numbers of corresponding samples are given on top of each bar; there are more zooplankton than phytoplankton samples available. Species identified as *Ceratium lineatum* during MUSE-2000 were removed from the *Ceratium* counts shown here because that species is non bioluminescent; most *Ceratium* species were not identified beyond genus. Small jellies include Physonect, Calycophoran, Hydromedusa, and *Beroe*. Additional counts (not represented here) are available for non-bioluminescent zooplankton and dinoflagellates as well as diatoms.

duration and intensity (hereafter flash kinetics) are taxon-specific and can be used to discriminate between taxa either directly (Johnsen et al., 2014) or via their impact on time series properties (Moline et al., 2009). Bioluminescence is very common throughout the water column, with 76% of marine animals observed at depths between 100 and 4000 m off California (planktonic or not) having bioluminescent capability (Martini and Haddock, 2017). In the upper ocean, small plankton communities include several bioluminescent species (Fig. 1); the most commonly encountered bioluminescent organisms are dinoflagellates (auto- and heterotrophic). Other bioluminescent taxa include larvaceans (appendicularians), copepods, euphausiids (krill), and small jellies (ctenophores and small medusae) (Haddock et al., 2010); their concentrations are typically 2–3 orders of magnitude less than for bioluminescent dinoflagellates (Fig. 1).

Because of the variety of bioluminescent species spanning phytoplankton (autotrophic dinoflagellates), small heterotrophic protists (heterotrophic dinoflagellates, radiolarians) and zooplankton (copepods, krill, and small gelatinous zooplankton), bathyphotometers present a unique opportunity to study plankton communities, their taxonomic composition and phytoplankton/zooplankton interactions in the sea. Efforts to move beyond bulk bioluminescence and to partition bioluminescence into taxonomic groups include light budgets, which require coinciding plankton counts (e.g., Marcinko et al., 2013a; Lapota, 2012a, 2012b), taxon discrimination using flash kinetics (Johnsen et al., 2014; Cronin et al., 2016) and time-series analysis (Moline et al., 2009). In coastal regions where the concentration of bioluminescent organisms is often high enough that flashes merge and become indistinguishable, methods based on flash kinetics cannot be used. To overcome this issue, here we propose a novel time series analysis method that exploits differences in concentration and flash intensity between taxa to define bioluminescence proxies for dinoflagellates, copepods, larvaceans, and small jellies. Combined with simultaneous measurements of fluorescence, these proxies can be extended to characterize communities of autotrophic and heterotrophic dinoflagellates, and other phytoplankton such as diatoms.

The paper is organized as follows. Section 2 presents the fluorescence and bioluminescence datasets, a modeling exercise used to investigate the impact of concentration and flash kinetics on the bioluminescence signal, the proxy calculation method, and its application to three field campaigns during which *in situ* plankton counts were collected alongside matching fluorescence/bioluminescence time series. Section 3 validates the proxies against *in situ* counts and presents results during the AOSN-2003 field campaign. Section 4 discusses situations when proxies may or may not be valid, and conclusions are offered in Section 5.

2. Datasets and methods

2.1. Fluorescence and bioluminescence sensors

The plankton proxies are based on bioluminescence and fluorescence measured by autonomous sensors onboard AUVs or deployed from ships. Bioluminescence and fluorescence are both light emissions by organisms, the main difference being that bioluminescence is produced by the organism itself through a chemical reaction, while fluorescent molecules do not produce their own light but absorb and reemit

photons originating from an external source (Haddock et al., 2010). Because coastal bioluminescence is dominated by dinoflagellates (Lapota et al., 1988; Moline et al., 2009; Marcinko et al., 2013b) whose bioluminescence is strongly inhibited during the day (Marcinko et al., 2013a), all datasets were restricted to nighttime (1 h after sunset to 1 h before sunrise).

Bathyphotometers (BPs) measure the "bioluminescence potential" of organisms (hereafter bioluminescence) by pumping seawater into a detection chamber, mechanically stimulating bioluminescent plankton, and detecting their light emission with a photomultiplier tube. The Multipurpose Bioluminescence Bathyphotometer (MBBP, Herren et al., 2005), later commercialized by WET Labs as the Underwater Bioluminescence Assessment Tool (UBAT, http://www.seabird.com/ubat), was specifically designed to sample highly dynamic coastal communities by providing 1 Hz resolution (later increased to 60 Hz). A complete description of the instrument, calibration and tests can be found in Herren et al. (2005). In the MBBP where residence time within the BP chamber (~10 s) exceeds the flash decay time, bioluminescence (B, in ph s^{-1}) can be related to plankton concentration as

$$B = [BLS] \times F \times TMSL \quad (1)$$

where [*BLS*] is the concentration of bioluminescent sources in L^{-1}, F the flow rate in L s^{-1} and *TMSL* the species-dependant, time-integrated Total Mechanically Stimulable Light in ph per individual (Latz and Rohr, 2013). As a consequence, B / F (bioluminescence expressed in ph L^{-1}, hereafter termed *BL*) is proportional to concentration for a given species (see Table 1 for a list of mathematical acronyms).

Fluorescence has been used for over 50 years to monitor chlorophyll concentration (Lorenzen, 1966) and represents a proxy for phytoplankton biomass (e.g., Boss and Behrenfeld, 2010). The relationships between fluorescence, chlorophyll concentration, and phytoplankton biomass are functions of light via quenching (depressed fluorescence at high irradiance) and photoacclimation (increased ratio of phytoplankton carbon to chlorophyll and fluorescence with irradiance), and also functions of phytoplankton physiological status and community composition (e.g., Dickey, 1988). By only considering nighttime data, variability due to photoacclimation and quenching is minimized, and we use fluorescence as a proxy for autotrophic phytoplankton biomass.

2.2. Simulated bioluminescence time series

The bioluminescence signal measured by BPs integrates light emitted by dinoflagellates and different types of zooplankton (copepods, krill, larvaceans, and small jellies; Fig. 1). Generally speaking, zooplankton emit bright flashes (> 10^{10} ph s^{-1}) while most dinoflagellate species only emit flashes < 10^{9} ph s^{-1} (Table 2). Characterizing flash intensity for different taxa from the literature is difficult at best, as species, methods, and organism physiological status may not be directly comparable across studies and these often report *TMSL* rather than flash intensity. Studies that include both zooplankton and dinoflagellates are rare and support zooplankton having higher flash intensity (Cronin et al., 2016) and *TMSL* (Buskey and Swift, 1990; Swift et al., 1995) than dinoflagellates (Table 2).

Using this basic premise of rare, bright zooplankton flashes and numerous, weak dinoflagellate flashes, we simulated bioluminescence time series by representing and summing the contributions of dinoflagellates and zooplankton. The goal was to develop the proxies and to investigate the effect of various parameters on the bioluminescence signal, such as flash kinetics and dinoflagellate/zooplankton concentration. The method for simulation is a 4-step process: (1) define a unit flash for each population (Fig. 2a), (2) for each population, randomize the flash distribution over time based on bioluminescent source concentration ([*BLS*]), (3) generate the corresponding bioluminescence time series by summing the unit flashes (Fig. 2b,c), and (4) sum the individual bioluminescence time series (Fig. 2d, black line). The unit flashes were parameterized following published values (Table 2) and tuned to represent the characteristics of a measured bioluminescence time series (Fig. 3a). Details are given in Appendix A regarding (1) the definition of unit flashes as a function of *TMSL*, flash duration and/or flash intensity, and (2) the randomization of time steps as a function of [*BLS*] (equal to concentration if each organism flashes exactly once within the BP chamber).

The simulated time series displayed in Fig. 2d (black) was generated using plankton concentrations measured at a surface sample collected during the AOSN-2003 field campaign (see Section 2.5). Comparison with a bioluminescence time series measured by the bathyphotometer at the same location (Fig. 3a) indicates that the simulated time series successfully represents the characteristics of the measured time series (Table 3), validating the method. Fig. 2 highlights how, in coastal areas, dinoflagellate concentrations are often high enough that their relatively weak flashes blend together, generating a bioluminescence background (Fig. 2c). By contrast, the bright flashes emitted by zooplankton (Fig. 2b) remain distinct in the combined time series (Fig. 2d). These characteristics are exploited by the proxy calculations presented below.

Table 1
Acronyms for mathematical variables.

B	Bioluminescence (measured)	ph s^{-1}
F	Flow rate	L s^{-1}
BL	Bioluminescence expressed per liter (= *B* / *F*)	ph L^{-1}
[BLS]	Bioluminescent source concentration (equal to concentration if each organism flashes once within the chamber)	L^{-1}
TMSL	Total Mechanically Stimulable Light	ph individual^{-1}
min_bg	Minimum bioluminescence background	ph s^{-1}
med_bg	Median bioluminescence background	ph s^{-1}
bg_BL	Minimum bioluminescence background expressed per liter (= *min_bg* / *F*)	ph L^{-1}
fluo	Fluorescence	raw units
ratioAdinos	*bg_BL* / *fluo* ratio for a given population of autotrophic dinoflagellates	dimensionless

2.3. Bioluminescence proxies

Methods identifying species from flash kinetics (e.g., Cronin et al., 2016) cannot be applied to typical coastal time series as individual flashes cannot be isolated (e.g., Fig. 3a). Instead, the proxy calculation is based on the basic premise represented in Fig. 2: the bioluminescence background is generated by dinoflagellates (Fig. 2c), while individual flashes are generated by zooplankton (Fig. 2b).

Background and flashes are estimated in a 3-step process detailed in Appendix B (Fig. 2d and 3). Briefly, the background representing the mean dinoflagellate bioluminescence is first calculated using a median sliding window method (*med_bg*, blue line). Second, an envelope is defined to capture the range of variation of the dinoflagellate signal (teal shading): the bottom limit (*min_bg*, teal line) is obtained using a minimum sliding window method, and the upper limit defined by symmetry around *med_bg* (see Appendix B). The assumption is that flashes within the envelope are generated by dinoflagellates while flashes above are generated by zooplankton. Third, flashes above the envelope are identified (stars) and their intensity defined relative to *med_bg*. To avoid very dim flashes when *min_bg* is low (e.g., Fig. 3b), a minimum envelope value of 1.5×10^{10} ph s^{-1} was set, corresponding to an approximate lower limit for zooplankton flash intensity. Flashes are further categorized into "low" and "high" intensity (yellow and red stars, respectively), as separated by a 10^{11} ph s^{-1} threshold (see Appendix B and Fig. B2).

Dinoflagellate and zooplankton proxies are defined as follows. The dinoflagellate proxy is *min_bg* divided by the flow rate (see Eq. (1)), termed *bg_BL*. *Min_bg* rather than *med_bg* was chosen because *med_bg* is more sensitive to zooplankton when their concentration is high (further discussed in Section 4.1). We consider that *bg_BL* is a proxy for all

Table 2
Published flash kinetics for species commonly observed in Monterey Bay, either measured or reported as "most probable value" (averaged when several species were reported in the same paper, excluding larval stages). This table supports the concept that zooplankton bioluminescence is higher than for dinoflagellates, noting that studies may not be directly intercomparable as they represent different regions, species and organism physiological status. Studies that include both zooplankton and dinoflagellates species support zooplankton having higher flash intensity **(21)** and *TMSL* **(10, 14)** than dinoflagellates. See text and Appendix A regarding the last two entries, * indicates numbers inferred from Fig. 3a. *Gonyaulax polyedra* is now placed in the genus *Lingulodinium*, and *Gonyaulax catenella / acatenella / tamarensis* are now placed in the genus *Alexandrium*. Flash duration is typically defined for B > 3% of flash intensity **(15)** and was approximated for **(20)** and **(21)** as 2 × Tmax (time until the emission reached maximum). The relationship between *TMSL* (Total Mechanically Stimulable Light; ph $cell^{-1}$) and quantum emission (/flash, ph $flash^{-1}$) depends on the number of flashes per cell, ~2–3 for *Ceratium* and *Lingulodinium* (see **(16)**). References: **(1)** Esaias et al. (1973), **(2)** Morin (1983), **(3)** Galt and Sykes (1983), **(4)** Lapota and Losee (1984); **(5)** Galt et al. (1985), **(6)** Galt and Grober (1985), **(7)** Herring (1988), **(8)** Lapota et al. (1989), **(9)** Batchelder and Swift (1989), **(10)** Buskey and Swift (1990), **(11)** Batchelder et al. (1992), **(12)** Buskey (1992), **(13)** Herring et al. (1993), **(14)** Swift et al. (1995), **(15)** Latz and Jeong (1996, their Tables 4 & 5), **(16)** Latz et al. (2004), **(17)** Lapota (2012b), **(18)** Craig and Priede (2012), **(19)** Valiadi and Iglesias-Rodriguez (2013), **(20)** Johnsen et al. (2014), **(21)** Cronin et al. (2016).

	Genus (% biolum species from **(19)**)	*TMSL* (ph $cell^{-1}$, *ph* $flash^{-1}$)	flash intensity (ph s^{-1})	flash duration(ms)
Autotrophic dinoflagellates	*Ceratium* (5%)	~3×10^8 **(1)** 5.3×10^8 **(10)** 5.4×10^8 **(11)** 3×10^8 **(14)** 4.8×10^8 **(17)** *(/flash)* 10^8 ***(4)*** *(/flash)* 9.7×10^7 ***(8)*** *(/flash)* 1.1×10^8 ***(18)***	3×10^8 **(4)** 1.1×10^9 **(16)**	180–270 **(4)** 239 **(16)** 200 **(18)**
	Alexandrium (23%)	~5×10^7 **(1)** 10^7 **(19)**		
	Lingulodinium (50%)	2.4×10^8 **(17)** *(/flash)* 1.9×10^8 ***(18)***	1.9×10^8 **(16)**	100–150 **(16)** 100 **(18)** 130–150 **(19)**
Heterotrophic dinoflagellates	*Protoperidinium* (11%)	2.1×10^9 **(10)** 2×10^9 **(11)** 10^9 **(13)** 1.9×10^9 **(14)** 2.8×10^9 **(17)** *(/flash)* 2.5×10^9 ***(8)***	2.6×10^9 **(15)** 10^9 **(21)**	135 **(15)** ~160 **(21)**
Larvacean	*Oikopleura*	3×10^{11} **(9)** 9.3×10^{10} **(10)** 5×10^{11} **(13, 5)** 10^{11} **(11)** 5.6×10^{11} **(12)**	10^9 **(2)** up to 1.5×10^{12} **(6)**	138 **(2)** 278 **(3)** ~150 **(5)**
Copepod	*Metridia*	9.5×10^{10} **(14)** 7.1×10^{10} **(9)** 1.4×10^{12} **(12)** *(/flash)* 3.44×10^{12} ***(18)*** *(/flash)* 1.2×10^{11} ***(8)***	6.4×10^{12} **(7)** 2.1×10^9 **(20)** 6.5×10^9 **(21)**	6700 **(18)** ~400 **(20)** ~260 **(21)**
	Oncaea	4.2×10^9 **(13)**	6.7×10^8 **(13)**	~130 **(13)**
Euphausiid	*Thysanoessa*	2×10^{11} **(9)** 9.4×10^{10} **(10)** 4×10^9 **(12)** 1.1×10^{11} **(14)** *(/flash)* 4×10^9 ***(8)***	2.5×10^{10} **(21)**	~440 **(21)**
	Nyctiphanes	*(/flash)* ~ 10^{11} ***(4)***	1.75×10^{10} **(4)**	~3000–7000 **(4)**
Ctenophore	*Beroe*		10^{11} **(20)** 2×10^{11} **(21)**	100–1600 **(2)** ~2200 **(20)** ~1400 **(21)**
Modeled dinoflagellates		6×10^8 *	5.4×10^9	250
Modeled zooplankton		10^{10}	4.4×10^{10} *	500

dinoflagellates as well as bioluminescent dinoflagellates, because both are highly correlated ($r = 0.52$, $p < 0.01$ for the dataset displayed in Fig. 1; $r > 0.8$ for SPOKES-2002 and AOSN-2003 when considered separately). Zooplankton proxies are based on flashes: the number of flashes per liter is used as a proxy for larvaceans (low intensity flashes) and copepods (high intensity flashes) while the maximum flash intensity is used as a proxy for small jellies. The rationale is that (1) larvacean flashes are dimmer than other types of zooplankton including copepods, (2) larvacean and copepods are common enough where a flash intensity threshold can be determined from sensitivity analysis (see Appendix B), and (3) while jellies are brightest and could theoretically be determined using another flash intensity threshold, they are too rare for this threshold to be determined but their presence should be indicated by very bright flashes.

Proxy calculations were applied to the simulated time series (blue/teal lines and yellow stars in Fig. 2d) to assess how successful the method is in separating the dinoflagellate and zooplankton signals. The resulting proxies do capture the correct dinoflagellate bioluminescence ($med\_bg = 4.2 \times 10^{10}$ ph s^{-1}, to be compared with the prescribed mean dinoflagellate bioluminescence of 3.9×10^{10} ph s^{-1}) and zooplankton flash concentration (2.25 flashes L^{-1} compared to the prescribed zooplankton concentration of 2.13 L^{-1}). Most of the simulated zooplankton flashes (Fig. 2b) were picked up by the proxy processing (Fig. 2d, yellow stars). A few were not (merging flashes counted as one) and some flashes were identified that belonged to the dinoflagellate rather than zooplankton time series (e.g., first yellow star), but overall the proxies succeeded in separating the simulated dinoflagellate and zooplankton signals.

2.4. Dinoflagellates and other phytoplankton

Fluorescence (*fluo*) is used in conjunction with the dinoflagellate

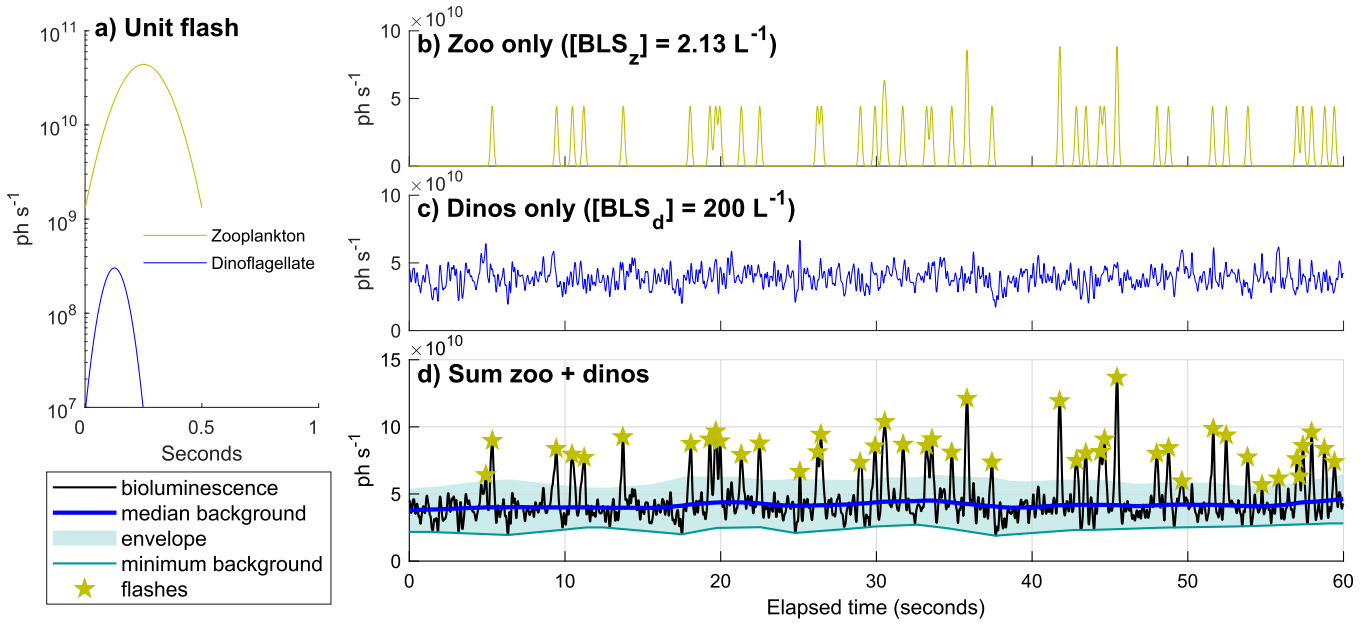

Fig. 2. Example of simulated bioluminescence time series. Flash kinetics (a) were chosen as typical of dinoflagellates (low intensity, short duration) and zooplankton (high intensity, longer duration) following Table 2 and calculations based on Eq. (1) (see Appendix A). The concentrations of bioluminescent sources ([*BLS*]) correspond to dinoflagellate and zooplankton concentrations in Fig. 3a; the zooplankton number was increased by considering that each larvacean corresponds to 5 *BLS* (luminescent inclusions in the house, Galt and Grober, 1985). The time series are separately constructed for zooplankton (b) and dinoflagellates (c) by calculating the average temporal interval between flashes based on concentration and a given flow rate (326 mL s^{-1} as in Fig. 3a), randomizing the time steps when flashes peak, and summing the individual flashes. The sum of the dinoflagellates and zooplankton time series (d, black) qualitatively and quantitatively captures the type of variability measured by the BP (Fig. 3a, see Table 3). Blue/teal lines and yellow stars are proxies computed on the simulated time series (Section 2.3). (For interpretation of the references to colour in this figure legend, the reader is referred to the web version of this article.)

proxy *bg_BL* to refine the dinoflagellate proxy into autotrophic (high fluorescence) and heterotrophic (low fluorescence) populations (Fig. 4a). When bioluminescence is low and fluorescence high, non-dinoflagellate phytoplankton dominate. These can include diatoms, flagellates, prymnesiophytes, picoplankton, etc. In coastal regions such as Monterey Bay, diatoms and dinoflagellates dominate the phytoplankton population and fluorescence signal (Chavez et al., 2017). Cases where fluorescence is high and bioluminescence low are thus attributed to diatoms in this paper, noting that other types of plankton can contribute to this signal particularly in other regions. While several dinoflagellate species are non-bioluminescent, bioluminescent and total dinoflagellate concentrations are highly correlated as explained above. By contrast, diatoms and dinoflagellates succeed each other, and are favored by different environmental conditions and less likely to cohabitate (Margalef, 1978; Smayda and Trainer, 2010).

Proxies for heterotrophic dinoflagellates (*h-dinos*), autotrophic dinoflagellates (*a-dinos*), and other phytoplankton (*a-other*, mostly diatoms in our datasets) are computed for a given fluorescence/bioluminescence dataset by assuming that the autotrophic dinoflagellate population (bioluminescent or not) is characterized by a constant *bg_BL / fluo* ratio, termed *ratioAdinos*. Details and equations are provided in Appendix B. Briefly, *ratioAdinos* is estimated from histograms as the most frequently observed *bg_BL / fluo* ratio. The *a-dino*, *h-dino* and *a-other* proxies are defined based on their location in the *bg_BL, fluo* space relative to *ratioAdinos* (Fig. 4b). These proxies, expressed in fluorescence units, are then normalized to the fluorescence 99th percentile value. “Dominance” of one plankton type is based on the highest proxy and can be understood as follows: *a-dinos* dominate when their fluorescence is higher than *a-other* fluorescence and their bioluminescence higher than *h-dino* bioluminescence; *a-other* dominate when their fluorescence is higher than *a-dino* fluorescence; and *h-dinos* dominate when their bioluminescence is higher than *a-dino* bioluminescence.

2.5. Application to field campaigns

Fluorescence and bioluminescence datasets, as well as *in situ* plankton counts, were collected during three field campaigns. These took place in Monterey Bay, California in Aug 24-Sep 2, 2000 (MUSE-2000), Aug 21–26, 2002 (SPOKES-2002), and Aug 10–16, 2003 (AOSN-2003). The objective of these field campaigns was to use a variety of platforms to obtain bay-wide distributions of biooptical parameters, along with corresponding plankton distributions, so they could be mapped to oceanographic features. As part of these efforts, fluorescence and bioluminescence sensors were deployed onboard ships, towfish and AUVs. Ship-based water samples for phytoplankton and zooplankton were collected using a CTD-rosette for phytoplankton and a 160 L Schindler trap for zooplankton (Fig. 1). Both methods allow for discrete sampling of a known volume of seawater from a well-constrained depth. Sampling varied across campaigns and days, following AUV surveys laid out in order to transition from nearshore to offshore environments. Sample depths ranged from the surface to ~40 m targeting zones above, at, and below the predominant thermocline, which was often associated with a band of high fluorescence. Samples were enumerated by microscopic examination. Both dinoflagellates and zooplankton (bioluminescent or not) were fully enumerated; orders of magnitude were estimated for diatoms and converted into approximate numerical values.

This paper focuses on two autonomous datasets and matching *in situ* counts: (1) bioluminescence measured by a BP attached to a shipboard Schindler trap (all campaigns), and (2) fluorescence and bioluminescence measured by a Dorado-class AUV (AOSN-2003). The first dataset is used to validate the bioluminescence proxies using plankton counts from all field campaigns (Section 3.1), and the second dataset is used for *h-dino/a-dino/a-other* proxy calculation (Section 3.2) and further analysis of the entire set of proxies (Section 3.3). Even though validations of the AUV proxies using shipboard samples is complicated by space and time lags, the AUV dataset was chosen because the *h-dino/a-*

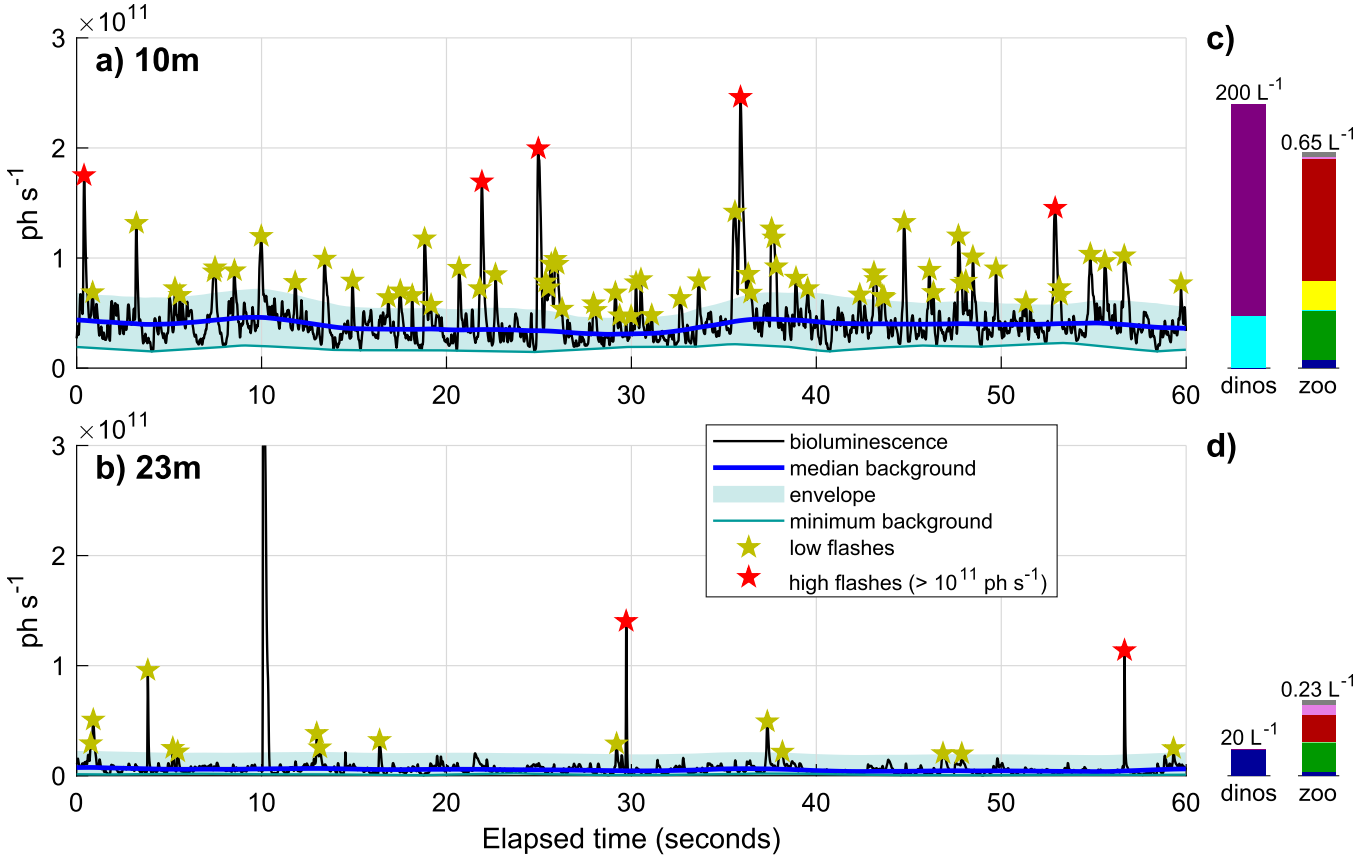

Fig. 3. Example of 60 Hz bioluminescence time series measured on Aug 15, 2003 (AOSN-2003 field campaign). The black line represents one minute of bioluminescence measured for a surface (a, 10 m) and subsurface (b, 23 m) sample at the same station. The proxies are indicated by blue/teal lines (dinoflagellate background bioluminescence) and stars (zooplankton flashes); blue shading highlights the bioluminescence envelope (dinoflagellate bioluminescence range of variation). The red star for the flash observed near 10 s in (b) is not visible because the flash peak (5.15 10^{11} ph s^{-1}) exceeds the range of the figure. The concentration and composition of bioluminescent plankton based on matching *in situ* samples is given on the right (c and d, see Fig. 1 for the color legend, y-axis are identical between 10 m and 23 m samples but different between dinoflagellates and zooplankton).

Table 3
Comparison of measured (Fig. 3a) and simulated (Fig. 2d) bioluminescence time series. Background bioluminescence, envelope and flashes are defined in Section 2.3. Note that the simulated flash concentration is dictated by the measured zooplankton concentration (see text) and is less than the flash concentration in the measured time series, which also has an impact on the variance. [1]A Hurst exponent close to 1 indicates a persistent time series (in the short term, the direction of change is retained). This is related to autocorrelation and thus strongly dependent on the time resolution. Computed using https://mathworks.com/matlabcentral/fileexchange/30076-generalized-hurst-exponent.

	Measured time series	Simulated time series
Mean (ph s^{-1})	4.5×10^{10}	4.6×10^{10}
Variance (ph s^{-1})	2.4×10^{10}	1.6×10^{10}
Autocorrelation at 50 ms (3 time steps)	0.85	0.89
Hurst exponent[1] (long-term memory of a time-series)	0.71	0.80
Background bioluminescence *med_bg* (ph s^{-1})	3.9×10^{10}	4.2×10^{10}
Ratio envelope/background $2 \times (med\_bg\text{-}min\_bg)/med\_bg$	1.06	0.87
Flash concentration (intensity $< 10^{11}$ ph s^{-1}, L^{-1})	3.28	2.25

dino/a-other proxies require both fluorescence and bioluminescence to be simultaneously measured. This rules out shipboard datasets because the CTD (fluorescence) and Schindler trap (bioluminescence) were sequentially deployed.

Different generations of MBBPs were used across campaigns, the main difference being the temporal resolution: 60 Hz for AOSN-2003, 1 Hz for MUSE-2000 and SPOKES-2002 (see Appendix B). This is a significant difference as typical flash durations can be 100–200 ms (Table 2), thus flashes are fully resolved with the 17 ms time step of the 60 Hz sensor but not with the 1 s time step of the 1 Hz sensors. The proxy method was directly applied to AOSN-2003 but had to be adapted for MUSE-2000 and SPOKES-2002. The *min_bg* bioluminescence was estimated using a similar sliding window technique. "Flashes" were identified as peaks in the 1 Hz signal above *min_bg* plus a given threshold specific to each field campaign (details in Appendix B). These thresholds, as well as other proxy parameters such as the sliding window used to define the background, were optimized through sensitivity tests based on correlations with *in situ* counts, where a range of values is attributed to a parameter while holding the others constant. The parameter resulting in the highest correlation with *in situ* counts was chosen (See Appendix B and Fig. B2).

3. Results

3.1. Comparison of bioluminescence proxies to in situ counts

The bioluminescent plankton communities during the three campaigns were diverse although they shared some characteristics (Fig. 1). Bioluminescent dinoflagellate concentration was higher near the surface; the main genera included *Protoperidinium*, *Alexandrium*, *Ceratium* and *Lingulodinium*. These genera include luminous and non-luminous species (Valiadi and Iglesias-Rodriguez, 2013), and we did not determine whether the sampled species were bioluminescent.

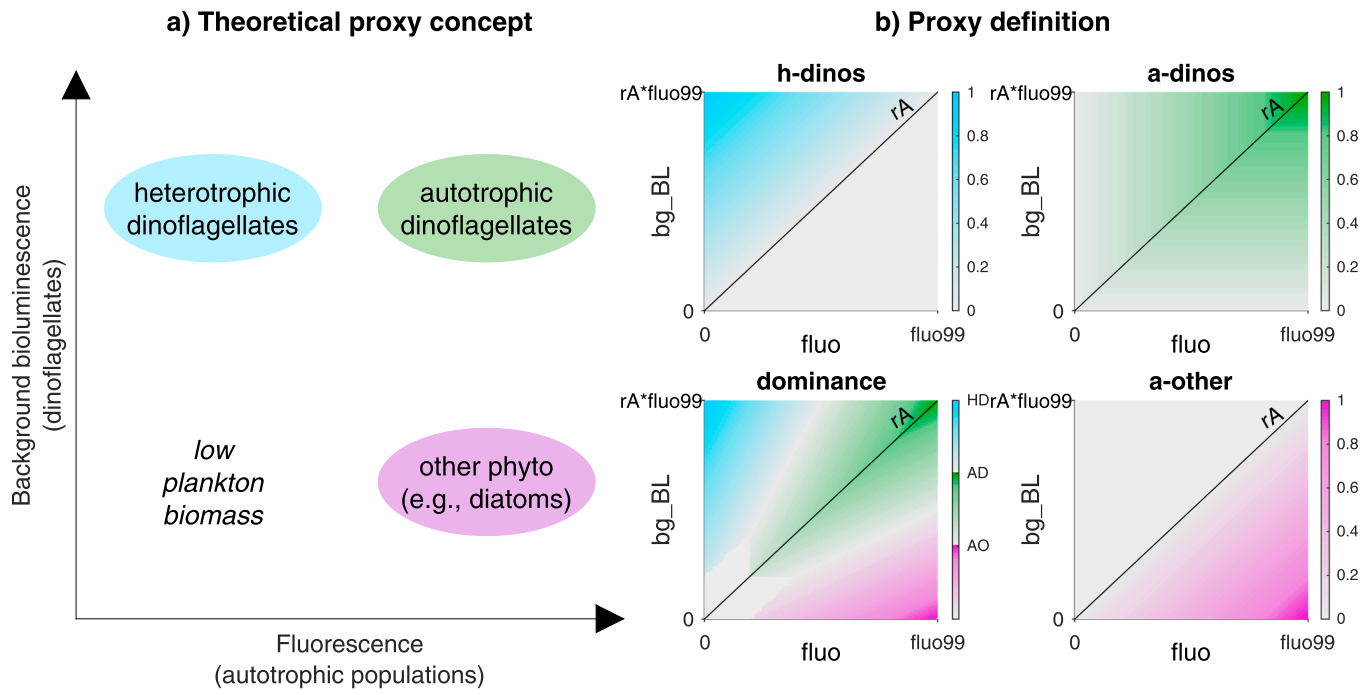

Fig. 4. Using fluorescence and bioluminescence to discriminate between non-dinoflagellate phytoplankton (mostly diatoms in Monterey Bay), autotrophic and heterotrophic dinoflagellates. (a) Schematic illustrating the basic concept: fluorescence is high for autotrophic populations, while background bioluminescence is high for dinoflagellates. Plankton characterized by high fluorescence and low bioluminescence are mostly diatoms in coastal ecosystems, but can include other non-dinoflagellate phytoplankton particularly in other regions. (d) Mathematical definition of *h-dino*, *a-dino* and *a-other* proxies and associated dominance in the *fluo, bg_BL* space (see equations in Appendix B). The slope of the black line is *ratioAdinos* (*rA*). The proxies are normalized such that a value of 1 corresponds to the 99th fluorescence percentile (*fluo99*). Labels for the dominance colorbar stand for *h-dinos* (HD), *a-dinos* (AD) and *a-other* (AO). (For interpretation of the references to colour in this figure legend, the reader is referred to the web version of this article.)

Table 4
Pearson correlation coefficients between bioluminescent plankton concentrations and 60 Hz bioluminescence proxies from the Schindler trap dataset (60 Hz is only available for AOSN 2003). "n.s." indicates correlations non-significant at the 5% level, * correlations significant at the 1% level, ** at the 0.1% level, bold expected correlations. (*) correlation with samples collected at the BP exhaust: r = 0.81** (N = 18).

	Background bioluminescence (ph L^{-1})	Low intensity flashes (nb L^{-1})	High intensity flashes (nb L^{-1})	Maximum intensity (ph s^{-1})
Dinoflagellates (N = 15)	**0.60**	n.s.	n.s.	n.s.
Larvaceans (N = 89)	0.48**	**0.46****	n.s.	n.s.
Larvaceans < 3.5 L^{-1} (N = 83)	*0.43***	***0.55*****	*n.s.*	*n.s.*
Copepods (N = 89)	n.s.	n.s.	**0.33***(*)	n.s.
Small jellies (N = 89)	n.s.	n.s.	n.s.	**0.31***

Table 5
Pearson correlation coefficients between bioluminescent plankton concentrations and 1 Hz bioluminescence proxies from the Schindler trap dataset. "n.s." indicates correlations non-significant at the 5% level, * correlations significant at the 1% level, ** at the 0.1% level, bold expected correlations (dinoflagellates with *bg_BL*, zooplankton with flashes). Numbers of samples are given for each campaign. The AOSN-2003 bioluminescence was adjusted using a 2.63 factor in the "combined" correlations to account for a change in BP (see Appendix B).

	Background bioluminescence (ph L^{-1})	Flash concentration (nb L^{-1})	
Dinoflagellates	**0.44****	n.s.	*MUSE-2000 (N = 84)*
	0.65**	n.s.	*SPOKES-2002 (N = 29)*
	0.52	n.s.	*AOSN-2003 (N = 15)*
	—	—	—
	0.49**	0.23*	*combined (N = 128)*
Zooplankton	0.36**	**0.34****	*MUSE-2000 (N = 96)*
	0.38	**0.49***	*SPOKES-2002 (N = 39)*
	0.39**	**0.45****	*AOSN-2003 (N = 89)*
	—	—	—
	0.18*	**0.29****	*combined (N = 224)*

Bioluminescent zooplankton was dominated by larvaceans followed by copepods; copepod concentration was higher in subsurface than surface samples. Bioluminescent zooplankton concentration was ~2–3 orders of magnitude lower than dinoflagellates.

The bioluminescence proxies were computed from time series measured by the Schindler trap BP and correlated to matching *in situ* plankton concentration (Tables 4 and 5). Only correlations significant at the 5% level ($p < 0.05$) are reported. Statistical significance was

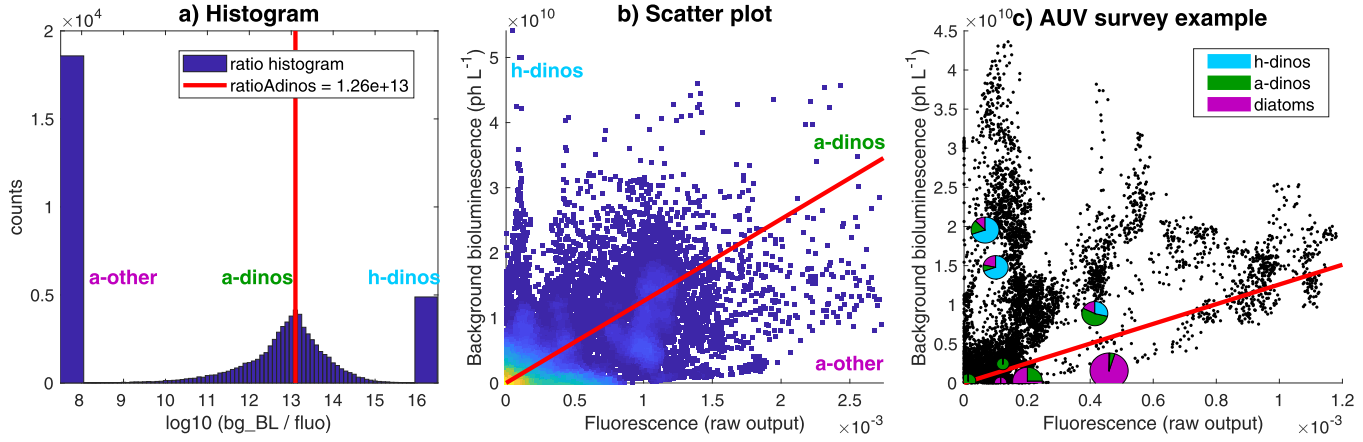

Fig. 5. Determination of *ratioAdinos* (ratio of background bioluminescence to fluorescence for autotrophic dinoflagellates) for the AOSN-2003 Dorado dataset. (a) Histogram of all measured nighttime *bg_BL/fluo* ratios during the campaign. The x-axis was set to highlight the most common ratio (*ratioAdinos*, red line); the left and right bars correspond to values less or equal to 8 and higher or equal to 16, respectively. (b) Scatter plot of *bg_BL* versus fluorescence during AOSN-2003 (colors indicate the density of data points). The red line highlights *ratioAdinos*. (c) Example of plankton composition as a function of matching AUV fluorescence and background bioluminescence averaged within a 30 s window around each sample location. Black dots represent the *fluo, bg_BL* dataset for the August 15–16, 2003 nighttime AUV survey. Pie charts are plankton samples taken along the AUV track and located in *fluo, bg_BL* space according to AUV measurement at the same location. Colors represent the plankton composition; the size is proportional to plankton concentration (dinoflagellates include both bioluminescent and non-bioluminescent species). The red line highlights *ratioAdinos* (note that axes are different between b and c). (For interpretation of the references to colour in this figure legend, the reader is referred to the web version of this article.)

estimated by assuming all samples are independent, which is a reasonable assumption for patchy biological populations. As an example, during AOSN-2003 samples were separated by ~3–4 km and > 1 h horizontally, 4–5 m and ~15 min vertically (for the closest depths). Simple calculations based on current velocities (~0.2–0.4 m/s horizontal and 10^{-4} to 10^{-3} m/s vertical, Shulman et al., 2015) and dinoflagellate vertical migration speeds (< 40 m day-1, Shulman et al., 2012) indicate that sampling occurred faster than plankton populations could travel. A possible exception are copepods, for which swimming speeds (~3–5 mm/s for *Metridia pacifica*, Wong, 1988) could approach vertical sampling speed for the closest stations; however, copepods are extremely patchy and mostly found deeper where vertical separation between samples increases. Repeat sections were rare and separated by several days.

Proxies computed for the AOSN-2003 field campaign (60 Hz data available) were able to separate between larvaceans, copepods and

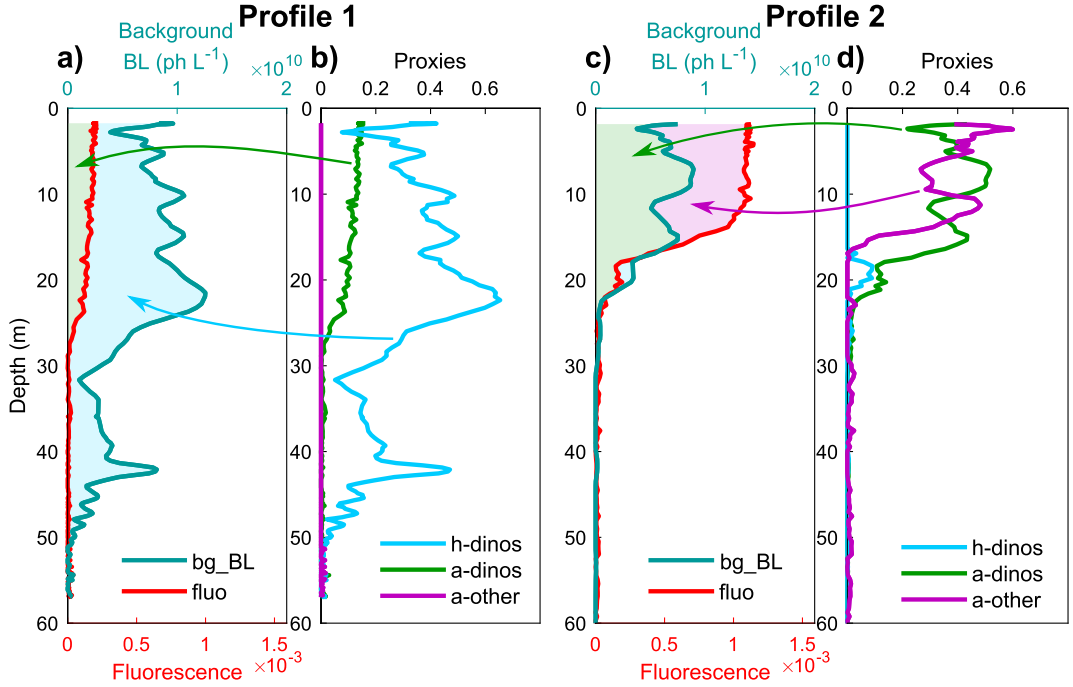

Fig. 6. Two examples of Dorado profiles on the August 15–16, 2003 nighttime survey (identified by blue triangles in Fig. 7) and associated proxies. Fluorescence and background bioluminescence (panels a & c) are used to calculate proxies for *h-dinos*, *a-dinos* and *a-other* (b & d) based on the relationships displayed in Fig. 4. The axes for *fluo* and *bg_BL* are set such that their ratio is equal to *ratioAdinos* when they superimpose; areas shaded in pink, green and blue in (a) and (c) thus correspond to *h-dinos*, *a-dinos* and *a-other* in (b) and (d) as indicated by the color arrows. More precisely, the lower of the *fluo* (red) and *bg_BL* (teal) lines is attributed to *a-dinos* (green); the difference between the *fluo* and *bg_BL* lines is attributed to *a-other* (purple) when *fluo* is higher (as in profile 2), and to *h-dinos* (soft blue) when *fluo* is lower (as in profile 1). (For interpretation of the references to colour in this figure legend, the reader is referred to the web version of this article.)

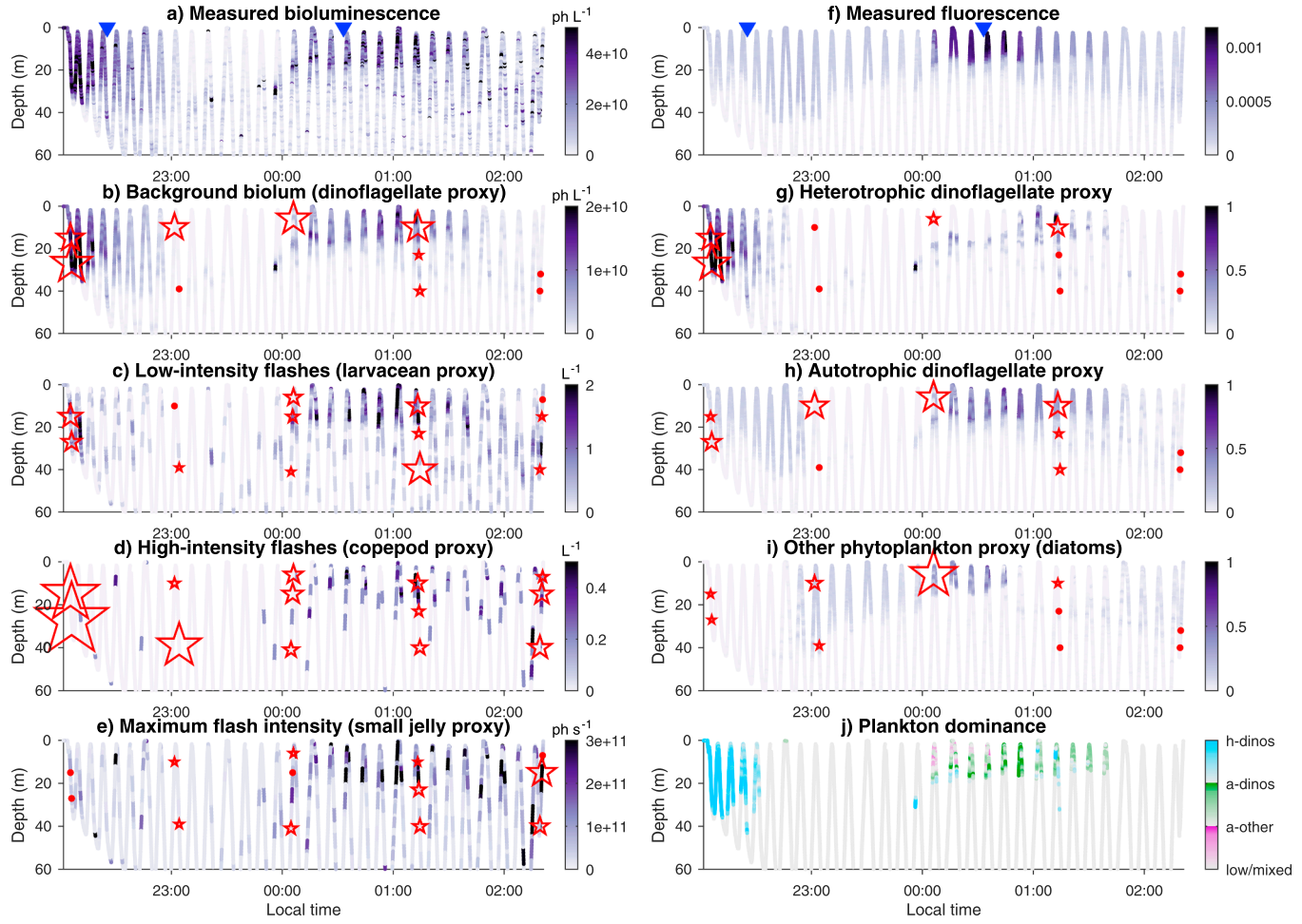

Fig. 7. Bioluminescence and fluorescence Dorado sections on the night of August 15–16, 2003 (top) and derived proxies (bioluminescence proxies on the left, fluorescence/bioluminescence on the right). The red stars/dots represent shipboard *in situ* counts along the same section (taken within 600 m of each location and 2 h of AUV sampling), including both bioluminescent and non-bioluminescent species. The stars are counts scaled for each variable, dots indicate where the count was 0. The scaling factor is identical for *a-dinos* and *h-dinos*, but different for diatoms, which were only qualitatively estimated. Plankton dominance in (j) is attributed to whichever has the highest proxy, and the value for the color mapping is the difference between the dominant and the next highest proxy (colorbars range: 0–0.4). When the value of the dominant proxy is < 0.2, dominance is set to 0 (low/mixed). Blue triangles in the top panels identify the two vertical profiles displayed in Fig. 6. The two high-copepod samples at the beginning contained no bioluminescent species. (For interpretation of the references to colour in this figure legend, the reader is referred to the web version of this article.)

small jellies as each zooplankton proxy was only significantly correlated with its target (bold numbers in Table 4). Background bioluminescence was correlated with both dinoflagellates and larvaceans, but more strongly with dinoflagellates. In general, correlations were higher for dinoflagellates (r = 0.60) than for zooplankton (r = 0.31–0.46); correlations for copepods and small jellies were significant at the 1% level but low (0.31–0.33). These zooplankton are rare and extremely patchy, and likely to exhibit avoidance behaviors, which may explain the low correlations. This is supported by the much higher correlation found for copepods when considering samples directly collected at the BP exhaust (r = 0.81, N = 18). Interestingly, correlations between larvaceans and low-intensity flashes, while relatively high (r = 0.46), were unexpectedly lower than correlations with *bg_BL* (r = 0.48). This is likely due to (1) larvaceans being highly correlated with dinoflagellates (r = 0.76, N = 14) and low-intensity flashes being correlated with *bg_BL* (r = 0.56, N = 89), and (2) larvaceans contributing to background bioluminescence when their concentration is high (discussed in Section 4.1). Indeed, excluding the few samples with larvacean concentrations greater than 3.5 L^{-1} increased the larvacean correlation with flashes to 0.55 and decreased the correlation with *bg_BL* to 0.43 (Table 4).

Only 1 Hz data was available for the other two campaigns, which does not allow flash resolution. The performance of proxies adapted for 1 Hz time series was assessed by computing both 1 Hz and 60 Hz proxies for AOSN-2003. Across the entire AUV nighttime dataset, their correlation is very high for *bg_BL* (r = 0.95) and lower for flashes (r = 0.76 for flashes per liter averaged over 15 sec windows), suggesting that 1 Hz is sufficient to resolve dinoflagellates but less so zooplankton. Consistent with this assessment, for AOSN-2003 the correlation between *bg_BL* and dinoflagellates only slightly decreased by using 1 Hz data (0.52 instead of 0.60, Tables 4 and 5). Even without flash resolution, 1 Hz bioluminescence proxies significantly correlated with the dinoflagellate and zooplankton concentrations during all three campaigns (Table 5). Correlations between 1 Hz *bg_BL* and dinoflagellate concentrations range from 0.44 to 0.65, and reach 0.49 when considering all three campaigns together. Correlations between zooplankton concentrations and the 1 Hz flash proxy ranged from 0.34 to 0.49, decreasing to 0.29 for the combined dataset. These low correlations are not surprising since 1 Hz time series do not resolve individual flashes. With the exception of zooplankton for MUSE-2000, zooplankton correlations with flashes are stronger than with *bg_BL*, and dinoflagellate correlations with *bg_BL* are always stronger than with flashes.

3.2. Fluorescence / bioluminescence proxies during the AOSN-2003 field campaign

H-dino, *a-dino* and *a-other* proxies were computed from the AUV Dorado nighttime dataset collected during the AOSN-2003 field campaign (August 10–16, 2003). For this dataset, fluorescence and bioluminescence are decoupled (r = 0.38). Fluorescence and background bioluminescence, while more strongly correlated, share less than half of their variance (r = 0.65) suggesting that the plankton community alternated between *h-dinos*, *a-dinos* and *a-other* (diatoms). The only parameter needed to define the proxies, *ratioAdinos*, was determined from the Dorado dataset by analyzing the ratio of the 60 Hz background bioluminescence and fluorescence, both regridded at a 1 Hz resolution. A histogram of the ratio clearly separates low (*a-other*), high (*h-dinos*) and intermediate (*a-dinos*) ratios (Fig. 5a). These intermediate ratios were most frequently around 1.26×10^{13}, chosen as *ratioAdinos* (unit undefined since fluorescence was raw data). Each point in the *fluo, bg_BL* space can be attributed to *h-dinos*, *a-dinos* or *a-other* populations based on its position relative to the *ratioAdinos* line (Fig. 4); *in situ* counts support this concept (Fig. 5c). The proxies were computed in fluorescence units and normalized to the fluorescence 99th percentile.

As an example, Fig. 6 displays two contrasting AUV profiles and their corresponding proxies. The first profile (Fig. 6a and b) is characterized by much higher *bg_BL* than *fluo* (with the *ratioAdinos* conversion), indicative of a community dominated by heterotrophic dinoflagellates as represented by the high *h-dino* proxy. The second profile (Fig. 6c and d) displays higher *fluo* than *bg_BL* in the top 15 m (with the *ratioAdinos* conversion), hence *h-dino* = 0 and *a-other* > 0. While lower, *bg_BL* remained relatively high. This suggests that autotrophic dinoflagellates were also present and that the phytoplankton community near profile 2 was a mix of diatoms and dinoflagellates (Fig. 6d). This was confirmed by samples taken nearby (Fig. 7, near midnight).

Correlations between AUV-based proxies and shipboard plankton counts are not straightforward because of time and space lags; moreover, only orders of magnitude were estimated for diatoms. Diatom (*a-other*) and dinoflagellate proxies were qualitatively compared with available plankton counts; an example is displayed in Fig. 7 for the last survey (August 15–16). The AUV track started near the Año Nuevo upwelling center and ended at an offshore location near 122.3°W, 36.8°N (see Fig. 8). This specific survey was chosen because 10 of the 15 AOSN-2003 phytoplankton samples correspond to this section. Fig. 7 illustrates how, from only two measured parameters (bioluminescence and fluorescence), a suite of proxies can be derived characterizing the phyto- and zooplankton communities. The proxies indicate that the community was dominated by heterotrophic dinoflagellates nearshore around 20 m (Fig. 7g, j), a mix of diatoms and autotrophic dinoflagellates in the middle of the transect and closer to the surface (Fig. 7h–j), larvaceans in similar locations as dinoflagellates but also deeper (Fig. 7c), and copepods and small jellies in patchy locations offshore, mostly in the top 30 m (Fig. 7d, e). *In situ* counts along the transect (red stars/dots) support these results, particularly for the diatom and dinoflagellate communities (right column). While zooplankton patterns are generally similar between proxies and *in situ* counts, the agreement is not as good as for diatoms and dinoflagellates. This was expected because of the patchiness of zooplankton populations and time/space lags (samples were taken within 600 m of the AUV track but on average an hour later). Relationships improve slightly when comparing the proxies to counts of bioluminescent species only, particularly for copepods at the beginning of the section (the 2 samples near 10 pm only had non-bioluminescent copepod species).

3.3. Analysis of the AOSN-2003 Dorado dataset

Combining all the Dorado surveys provides a picture of plankton communities in Monterey Bay during upwelling conditions and highlights the potential of the method (Fig. 8). A single map was built because winds were consistently upwelling-favorable (Shulman et al., 2011; Fig. 8a), suggesting that spatial variability was likely stronger than temporal variability. The proxies indicate that dinoflagellates dominated near shore while other phytoplankton (here diatoms) were

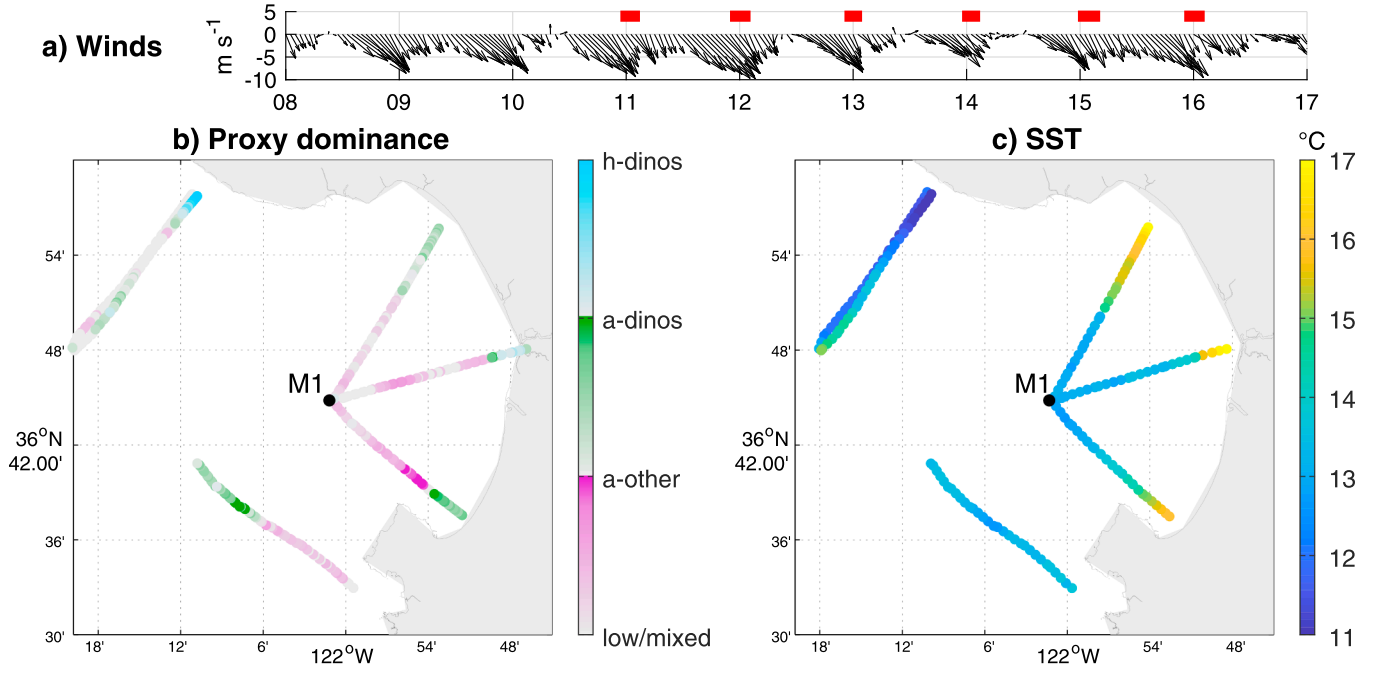

Fig. 8. Dorado nighttime surveys during the AOSN-2003 field campaign (Aug. 11–16). (a) Wind vectors measured at station M1, with Dorado surveys highlighted by red bars. Winds were upwelling-favorable the whole time. (b) Average proxies in the top 50 m were used to calculate plankton dominance by heterotrophic dinoflagellates (blue), autotrophic dinoflagellates (green) and other phytoplankton (diatoms, purple) following the same logic as Fig. 7j. Here the color bar range is 0–0.3. (c) Sea surface temperature defined as the point closest to the surface for each profile (generally in the top 2 m). The section displayed in Fig. 7 is located off Año Nuevo (north-westernmost track). (For interpretation of the references to colour in this figure legend, the reader is referred to the web version of this article.)

more abundant inside the bay (Fig. 8b). This plankton distribution mirrors the surface temperature measured by the vehicle (Fig. 8c) with dinoflagellates dominating in warm waters and diatoms in colder waters. This is consistent with the model presented by Smayda and Trainer (2010) in which diatoms bloom first when upwelling intensifies, then dinoflagellates bloom when upwelling relaxes. Spatially, this translates into diatoms dominating recently (cold) upwelled waters and dinoflagellates dominating older (warmer) waters as illustrated by Fig. 8. Dinoflagellate vertical migration could also contribute to the inshore/offshore difference in plankton composition, as dinoflagellates from the northern bay were able to avoid advection by the strong southward surface currents by migrating deeper, while non-migrating diatoms were advected (Shulman et al., 2011, 2012).

Average fluorescence, bioluminescence and proxy profiles provide additional information regarding the vertical distribution of different plankton types during AOSN-2003 (Fig. 9). Fluorescence peaked in the top 10 m and sharply decreased with depth, while bioluminescence was highest down to 20 m and slowly decreased through the water column (Fig. 9a). Bioluminescent flashes (zooplankton) remained numerous down to 100 m where their density was still ~25% of the surface density (Fig. 9b); copepods (high-intensity flashes) peaked deeper than larvaceans (low-intensity flashes). Flashes were responsible for the very high variability in the bioluminescence time series relative to fluorescence, as illustrated by the standard deviation in relation to the mean. By contrast, *bg_BL* (dinoflagellate proxy) was considerably less variable and slowly decreased with depth, becoming negligible below 50 m. The *h-dino*, *a-dino* and *a-other* proxies (Fig. 9c) suggest that heterotrophic dinoflagellates tend to occur deeper in the water column than phytoplankton (*a-dinos* + *a-other*). Phytoplankton vertical distribution was similar between autotrophic dinoflagellates and other phytoplankton (diatoms), although dinoflagellates remained high slightly deeper than diatoms.

4. Discussion

4.1. Validating the method: Insights from simulated time series

The proxies rely on the assumption that dinoflagellates' numerous low-intensity flashes merge to generate a bioluminescent background, whereas zooplankton emit infrequent high-intensity flashes above the background. Here we revisit this assumption using the simulated time series presented in Section 2.2 (Fig. 10). Time series were generated for varying concentrations of bioluminescent sources ([*BLS*]) and for a given plankton type characterized by its flash kinetics, here chosen to represent zooplankton (Fig. 2a). The goal was to analyze how the bioluminescence signal changes as a function of concentration for a given species, and to verify whether the proxies indeed correlate with plankton concentrations.

For very low concentrations ([*BLS*] < ~4 L^{-1}, e.g., Fig. 10a), the number of flashes (yellow) is proportional to [*BLS*] for simulated time series, following the theoretical dashed yellow line. In this case both *min_bg* (teal) and *med_bg* (dark blue) are close to 0. For higher concentrations ([*BLS*] > ~4 L^{-1}), the flash density becomes high enough where flashes start to merge (*med_bg* > 0, Fig. 10b). The flash proxy still increases with [*BLS*] until ~6–7 L^{-1} but becomes lower than theoretical values, and above ~6–7 L^{-1} becomes unreliable as it decreases with increasing [*BLS*] (Fig. 10d). Regarding the background, once flashes begin to merge and a background is generated (i.e. for [*BLS*] > 4 L^{-1}), *med_bg* increases with [*BLS*] and tracks the theoretical background computed from Eq. (1) (dashed blue line in Fig. 10d). By contrast, *min_bg* only becomes positive for [*BLS*] > ~20 L^{-1} (e.g., Fig. 10c) then also increases with [*BLS*] following *med_bg*. In the simulations, these thresholds are sensitive to the flash duration (here 500 ms) but not to flash intensity. For shorter flash duration thresholds are higher (~10 L^{-1} and 60 L^{-1} for a typical dinoflagellate flash duration of 200 ms instead of ~4 L^{-1} and 20 L^{-1}, not shown). To summarize, this exercise illustrates how [*BLS*] is correlated to flashes at low concentrations ([*BLS*] < ~6–7 L^{-1} for zooplankton), to *med_bg*

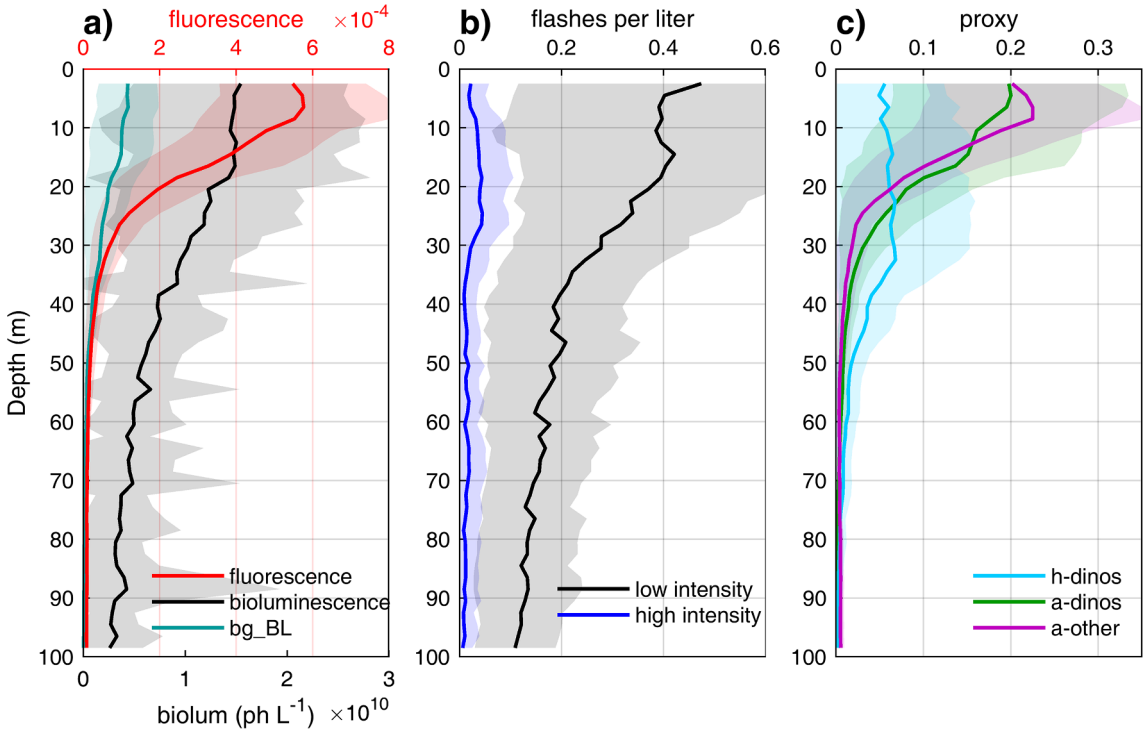

Fig. 9. Average vertical profiles for fluorescence, bioluminescence and derived proxies during the AOSN-2003 field campaign. The profiles were computed in 2 m bins, each averaging ~ 1500 data points except near the surface and 100 m where the AUV turns, sharply increasing the number of data points to > 5000. In (a), *bg_BL* is computed from *min_bg* (proportional to dinoflagellates but not representing dinoflagellate bioluminescence). The width of the shading represents the standard deviation for each profile.

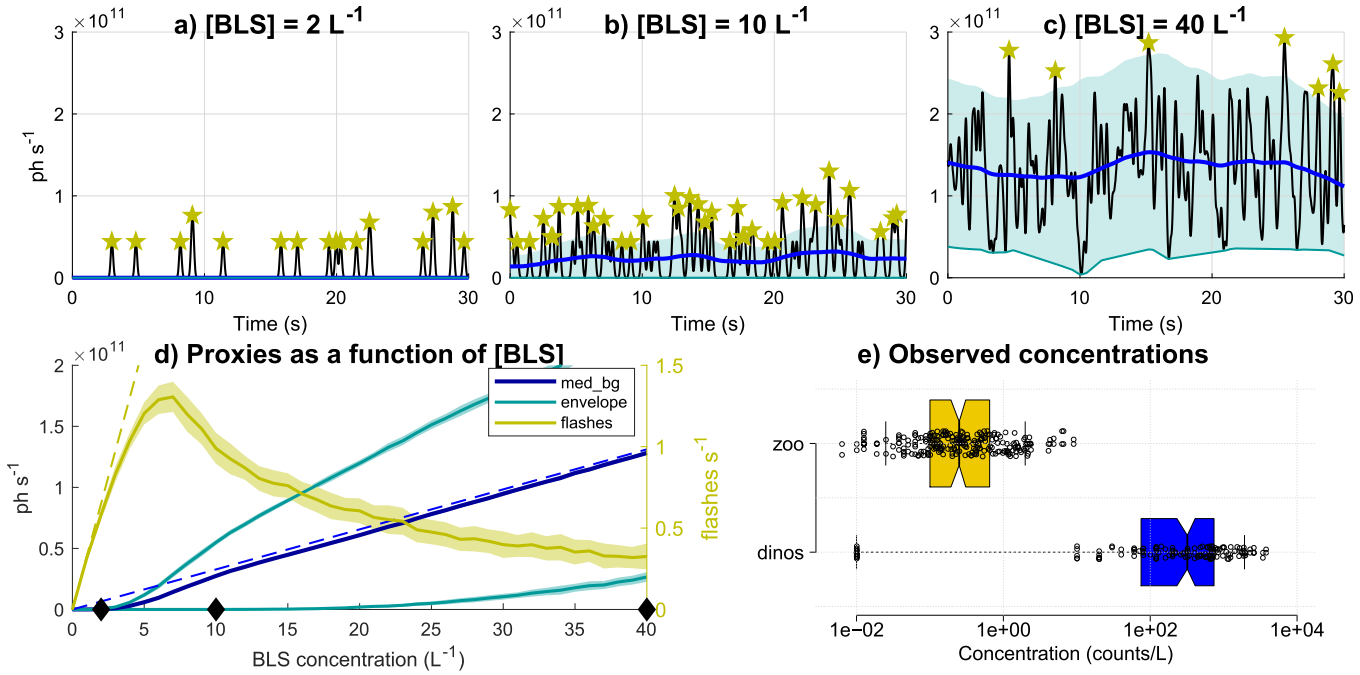

Fig. 10. Investigating the effects of cell concentration on the shape of the bioluminescence signal and the validity of proxies. Top panels: examples of simulated 60 Hz time series based on one plankton type (zooplankton) and increasing bioluminescence source concentrations ([*BLS*]). The corresponding proxies are displayed as blue lines and stars (see Fig. 2 for the legend; low/high intensity flashes were not separated and the minimum envelope value of 1.5×10^{10} ph $^{-1}$ was not applied). Bottom panels: (d) evolution of proxies as a function of [*BLS*], obtained by averaging results from 100 simulations for each [*BLS*] (shading represents +/− 1 standard deviation around the mean, very small except for flashes). Black diamonds indicate the concentrations for which example time series are displayed in top panels. Dashed lines are theoretical relationships: *[BLS]* × *F* for flashes (yellow) and *[BLS]* × *F* × *TMSL* for background (blue) where *F* is the flow rate (cf Eq. (1)). (e) Observed plankton concentrations during the 3 field campaigns (log scale), plot generated using BoxPlotR (http://shiny.chemgrid.org/boxplotr/). Data points are plotted as open circles; center lines show the medians; box limits indicate the 25th and 75th percentiles as determined by R software; whiskers extend to 5th and 95th percentiles (the 95th percentile for zooplankton is ~2 L^{-1}); the width of the boxes is proportional to the square root of the sample size (N = 139 for dinos, 233 for zoo). (For interpretation of the references to colour in this figure legend, the reader is referred to the web version of this article.)

except at very low concentrations (< ~4 L^{-1}), and to *min_bg* when concentrations are high enough ([*BLS*] > 20 L^{-1} for zooplankton, 60 L^{-1} for dinoflagellates) (Fig. 10d).

Fig. 10d can be used to assess the validity of the proxies based on observed concentrations (Fig. 10e). Zooplankton concentrations measured during the 3 field campaigns were ~0.25 L^{-1} and mostly below 2 L^{-1}. Zooplankton may flash several times and larvacean houses contain several bioluminescent inclusions, which could increase [*BLS*] to ~1–2 L^{-1} and mostly below 10 L^{-1}. For these concentrations, the flash proxy is proportional to [*BLS*] although it would underestimate zooplankton for high concentrations (> 4 L^{-1}). AOSN-2003 correlations supports this hypothesis by showing a increase in performance for the larvacean proxy when excluding samples with larvacean concentrations > 3.5 L^{-1}, also corresponding to bioluminescent zooplankton > 4 L^{-1} ("high BLzoo samples", 7% of the samples, Table 4).

The validity of the dinoflagellate proxy can also be estimated from Fig. 10d as a function of concentration. Measured bioluminescent dinoflagellate concentrations were most often > 100 L^{-1} , a situation where both *min_bg* and *med_bg* are proportional to [*BLS*] (Fig. 10d, noting that in dinoflagellate simulations with shorter duration flashes, *min_bg* becomes > 0 above ~ 60 L^{-1} instead of ~ 20 L^{-1}). Either *min_bg* or *med_bg* can be used as a dinoflagellate proxy since both are highly correlated (r = 0.96 in the AOSN-2003 AUV dataset). However, *med_bg* is sensitive to zooplankton above ~4 L^{-1} while *min_bg* only becomes > 0 at much higher zooplankton concentrations (~20 L^{-1}). *Min_bg* is thus a better dinoflagellate proxy as it is less likely to be "contaminated" by zooplankton.

A previous paper introduced the time series coefficient of variation (CV, standard deviation divided by mean) as a tool to separate between dinoflagellates and zooplankton (Moline et al., 2009). The simulated time series were used to assess how CV varies as a function of [*BLS*], similar to the results presented in Fig. 10. For a given plankton type characterized by its flash kinetics, CV decreases exponentially with [*BLS*] such that 1/CV is strongly correlated with [*BLS*] and the mean bioluminescence (r = 0.99 for simulations shown in Fig. 10). This is directly due to flashes merging when concentration increases, decreasing CV (visible in Fig. 10a–c for which CV = 2.3, 0.9 and 0.4, respectively). No correlations were found between CV and *in situ* plankton concentrations, also suggesting that CV is not an indicator of zooplankton or dinoflagellate concentration. However, when considering CV as a function of bioluminescence for dinoflagellates and zooplankton (from simulated time series with different flash kinetics), CV is indeed much higher for zooplankton than dinoflagellate populations (Fig. 11a). In the simulations, for typical concentrations CV was higher than 1 for zooplankton, lower than 1 for dinoflagellates, and about 3 times higher for zooplankton than dinoflagellates for a given bioluminescence value. These results justify the use of CV as a tool to separate between dinoflagellates and zooplankton as in Moline et al. (2009), noting that CV cannot be used as a proxy as it is inversely proportional to concentration. By contrast, the flash proxy presented here is also much higher for zooplankton than dinoflagellates, and is proportional to zooplankton concentration except for very high concentrations (Fig. 10d and 11b) so that it is a better zooplankton proxy.

4.2. Limitations of the plankton proxies

The results presented above support the use of bioluminescence- and fluorescence-derived variables as proxies for dinoflagellates, other phytoplankton such as diatoms, and different types of zooplankton. The proxies were validated using simple correlations with *in situ* plankton counts (Tables 4 and 5). These correlations, while significant ($p < 0.01$ except for dinoflagellates during AOSN-2003 where $p < 0.05$), remain relatively low particularly for zooplankton ($r < 0.5$). This suggests that quantitative

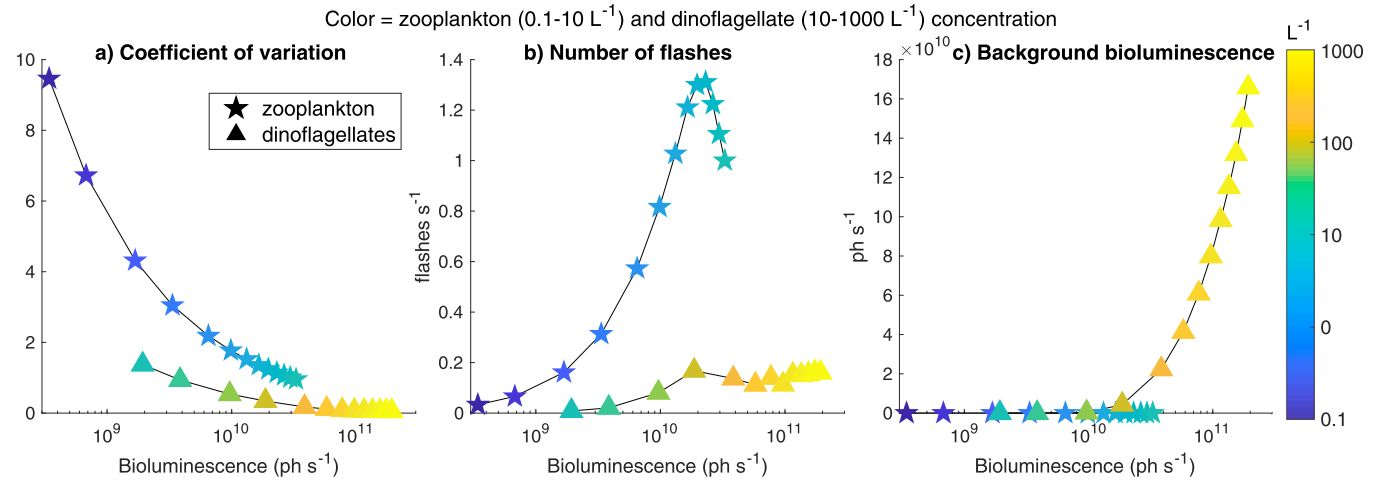

Fig. 11. Proxies as a function of bioluminescence for typical phytoplankton and zooplankton concentrations (from the simulated time series, unit flashes as in Fig. 2a). For each phytoplankton and zooplankton concentration (colors), 100 1-min simulated time series were generated and the corresponding bioluminescence and proxies values averaged: (a) CV, (b) flashes, (c) *min_bg*. For a given bioluminescence value, simulated zooplankton populations (stars) exhibit a higher CV than simulated dinoflagellate population (triangles); however, CV is inversely proportional to concentration (a). The flash proxy is proportional to simulated zooplankton concentration except for high concentrations ($[BLS] > 6\,L^{-1}$, b) and *min_bg* is proportional to simulated dinoflagellate concentrations except for low concentrations ($[BLS] < 100\,L^{-1}$, c). (For interpretation of the references to colour in this figure legend, the reader is referred to the web version of this article.)

relationships are lacking at this point and that the zooplankton proxies should be considered with caution, particularly for small jellies and to a lesser extent copepods. Because each proxy is only correlated with its target population (Table 5), the proxies should at least provide qualitative evidence of changes in concentration for a given population.

There are several caveats associated with the method; perhaps the most important is that while the proxies capture changes in populations and the relative dominance of *h-dinos/a-dinos/a-other* (e.g., Fig. 7), they cannot provide information on concentrations without proper calibration based on *in situ* counts. Intercomparisons between different instruments is difficult at best, as illustrated by the difference in bioluminescence measured by two generations of BPs during the AOSN-2003 campaign (see Appendix B). While in theory bioluminescence is a direct function of concentration, flow rate, and *TMSL* (Eq. (1)), in practice it also depends on pre-stimulation of organisms prior to reaching the BP chamber, and on the BP stimulation efficiency (Herren et al., 2005). Latz and Rohr (2013) systematically tested several BPs and found that these parameters vary with the BP design and the organisms tested, such that bioluminescence cannot be directly compared across instruments. In addition, which platform is used and how the BP is mounted can impact the signal as well, notably for zooplankton because of avoidance behavior. The bioluminescence proxies were primarily developed based on data measured by a 60 Hz BP deployed during AOSN-2003 and later commercialized as the WET Labs UBAT (http://www.seabird.com/ubat). The method could thus be applied to other UBAT datasets, although parameters such as the minimum envelope and flash threshold would need to be adjusted. While the proxies could be adapted to different BP/fluorometer combinations, direct quantitative intercomparisons of resulting proxies would be difficult. Within the same dataset, the proxies are expected to be proportional to the concentration of their target species, with a few caveats:

First, zooplankton proxies are only representative of the water being sampled by the BP, and may not be representative of local conditions because of organism patchiness and low concentrations. It is thus difficult to relate a water sample to the signal measured by the BP even when taken close in space and time. This is particularly true for copepods and small jellies, for which significant but low (r = 0.31–0.33) correlations were found. This issue is illustrated by zooplankton samples collected simultaneously from the Schindler trap and at the BP exhaust (N = 18). The correlation between the two sets of samples for copepod concentration was only 0.23, highlighting a strong small-scale variability. The correlation between the number of high-intensity flashes and bioluminescent copepods increased from 0.24 for the Schindler trap samples to 0.81 for the BP exhaust samples.

Second, the larvacean proxy (low-intensity flashes) becomes unreliable both at high larvacean concentrations (Fig. 10d) and at high dinoflagellate concentrations (high background that would mask larvacean flashes). This is not an issue for the copepod proxy, as their concentrations are unlikely to exceed the threshold for flash proxy validity (~6–7 L^{-1}, Fig. 10d), and their flashes are bright enough that only extreme dinoflagellate concentrations would generate a background high enough to mask them. The larvacean proxy is also likely confounded by the fact that larvacean bioluminescence originates from their house rather than from the animal itself (Galt et al., 1985). Galt and Grober (1985) found that bioluminescence varies as a function of animal size and number of luminescent inclusions in the house, such that the number of flashes associated with each larvacean may vary widely.

Last, the separation of *h-dinos*, *a-dinos* and *a-other* relies on the assumption that bioluminescent and non-bioluminescent dinoflagellates covary such that the ratio of fluorescence to bioluminescence in *a-dinos* populations (*ratioAdinos*) remains constant. This assumption is supported by the correlation between bioluminescent and total dinoflagellate species in our dataset (r = 0.52, p < 0.01 over the three field campaigns). Kim et al. (2006) also reported a synchronous increase in both bioluminescent and non-bioluminescent dinoflagellate species during a bloom, and Marcinko et al. (2013b) identified a number of studies that found positive associations between bioluminescence and total dinoflagellate concentration (bioluminescent or not). However, dinoflagellate communities can evolve over time, and *ratioAdinos* could for instance increase when the *a-dino* population shifts towards more bioluminescent dinoflagellates leading to an overestimate of *h-dinos* relative to *a-other*. Particularly in large datasets spanning very diverse communities, deviations from the average relationship are possible and would result in unreliable proxies.

5. Conclusions and perspectives

Using outputs from two autonomous sensors (fluorescence and bioluminescence), a suite of proxies can be derived characterizing the coastal plankton community including non-dinoflagellate phytoplankton (e.g., diatoms), autotrophic dinoflagellates, heterotrophic dinoflagellates, larvaceans, copepods, and small jellies. Bathyphotometers thus bring tremendous added value relative to fluorometers alone, by extending

biological representations from bulk phytoplankton to dominant functional group, and more importantly to the heterotrophic community. Applying the proxies to AUV surveys during a 2003 field campaign in Monterey Bay, California, offers a glimpse into the potential of the method. The calculations show how plankton populations overlap in places and differ in others (Fig. 7), relate to environmental conditions (Fig. 8), and display contrasting vertical distributions (Fig. 9).

The decoupling between fluorescence and bioluminescence provides information on the relative dominance of dinoflagellates and on phytoplankton/zooplankton interactions in the sea. This can have notable implications, for instance in monitoring harmful algal blooms. Coastal upwelling harmful species include 27 dinoflagellate species and only 1 diatom species (Trainer et al., 2010), although the toxic diatom *Pseudonitzschia* can reach high biomass in all upwelling systems. Several of the harmful (toxic or oxygen-depleting) dinoflagellate species are known to be bioluminescent, such as *Lingulodinium polyedrum*, *Ceratium fusus*, *Alexandrium catenella*, and *Noctiluca scintillans*. Bioluminescence has previously been proposed as a tool to monitor harmful species (Kim et al., 2006) but there is at present no known method that can determine whether a dinoflagellate bloom is harmful or not from their bioluminescent emissions.

Zooplankton research is currently largely limited to sampling by net tows and to imaging and acoustic surveys. In recent years, acoustic sensors have been integrated onboard AUVs (e.g., Powell and Ohman, 2012; Moline et al., 2015) but these datasets remain limited. By contrast, bathyphotometers have been deployed for years if not decades. The Dorado AUV has been operating in and near Monterey Bay since 2003, now representing a 15-year time series of concurrent fluorescence and bioluminescence measurements. The corresponding proxies could shed light on zooplankton temporal and spatial patterns, interactions with phytoplankton, and environmental forcing. While proxies do not represent a direct measure of zooplankton concentration nor biomass, they can provide valuable information on the community's spatio-temporal variability. The method presented here represents a novel effort to go beyond direct measurements to visualize zooplankton, in line with other studies attempting to infer its distribution from space (Messié and Chavez, 2017), from coupled physical/biological models (Santora et al., 2013), and from next generation DNA sequencing methods (Harvey et al., 2017). To help make the proxies more readily tested and adopted by the community, example datasets and the toolbox of programs necessary to compute the proxies are available online at https://bitbucket.org/messiem/toolbox_BLprocess.

Acknowledgements

This work was supported by the David and Lucile Packard Foundation, and by ONR Grant N00014-00-1-0842 to S.H. I.S. was supported through the US Naval Research Laboratory under program element 61153 N. We appreciate the support of Hans Thomas and the AUV operations team, SeaBird WET Labs for the loan of the instrument, and John Ryan and Jodi Brewster for early assistance with data processing toolboxes.

Appendix A: Details of generating the simulated time series

(1) Unit flash definition

Individual flashes are represented using a simple Gaussian shape (Fig. 2a), cut such that the minimum is 3% of the maximum following Latz and Jeong (1996)'s definition of flash duration. A non-symmetrical skewed Gaussian may be more representative of bioluminescent flashes, particularly for copepods (e.g., Cronin et al. (2016), their Fig. 1) but requires an additional parameter and does not change the results. Flashes are defined using 3 parameters: maximum intensity, duration, and *TMSL*, assuming that *TMSL* is entirely emitted in one flash. Only 2 parameters can be set independently because duration and maximum intensity constrain the flash shape and thus the area below the curve (*TMSL*). Examples are provided in Fig. 2a where flashes were defined using the parameters listed in Table 2 (last 2 lines), estimated from Fig. 3a as follows. The dinoflagellate *TMSL* (6×10^8 ph cell^{-1}) was computed from Eq. (1) using B = 3.7×10^{10} ph s^{-1} (*med_bg* in Fig. 3a) and [*BLS*] = 200 L^{-1} (measured bioluminescent dinoflagellate concentration). The zooplankton flash intensity (4.4×10^{10} ph s^{-1}) was calculated as the average flash intensity for low-intensity flashes ($< 10^{11}$ ph s^{-1}). The duration was then tuned to represent published parameters (Table 2) and the shape of the bioluminescence time series (Fig. 3a), and the third parameter constrained by the first two.

(2) Flash randomization

The bioluminescence signal generated by dinoflagellates and zooplankton is modeled separately based on the concentration of bioluminescent sources ([*BLS*]). The time series are constructed by calculating the average number of flashes per time step $FL = [BLS] \times F \times dt$ (where F is the flow rate and dt the time step, here 1/60 s), then randomizing the flash distribution over time. The randomization method depends on *FL* as follows. If $FL < 0.5$ (i.e., less than one flash every 2 time steps, as is the case in Fig. 2b where $FL \sim 0.01$), the total number of flashes during the time series (N) is calculated as *FL* multiplied by the number of time steps, and N time steps are randomly chosen within the time series. This ensures that the number of flashes is exact, however, no more than one flash peaks on the same time step. Flashes still merge when the timing between their peaks is less than the flash duration (e.g., Fig. 2b near 20 s), sometimes even getting superimposed (e.g., near 35 s). When $FL > 0.5$, as is the case in Fig. 2c ($FL \sim 1.09$), the flash distribution is randomized using a truncated normal distribution centered at *FL* and with a standard deviation of $1/6 \times FL$, generated using the Matlab function randraw.m (https://mathworks.com/matlabcentral/fileexchange/7309-randraw). Zeros are added to the truncated normal distribution such that the distribution mean is also equal to *FL*. The 1/6 factor was visually chosen to best match measured bioluminescence time series. The truncated normal distribution was chosen instead of a Poisson distribution to permit the tuning of the standard deviation (1/6 factor).

Appendix B: Proxy calculation details

The proxy computation workflow for the AOSN-2003 Dorado dataset is summarized in Fig. B1 and consists of two steps: (1) dinoflagellate and zooplankton proxies are computed from the 60 Hz bioluminescence time series, (2) background bioluminescence and fluorescence are combined to calculate *h-dino*, *a-dino* and *a-other* proxies. Matlab programs to reproduce these calculations are available online at https://bitbucket.org/messiem/toolbox_BLprocess.

(1) Dinoflagellate and zooplankton proxies

The background bioluminescence is estimated using a sliding window method (5 s window for 60 Hz time series). The minimum background (*min_bg*) is obtained by taking the minimum value within each window, then applying an additional mean window smoothing on the resulting time

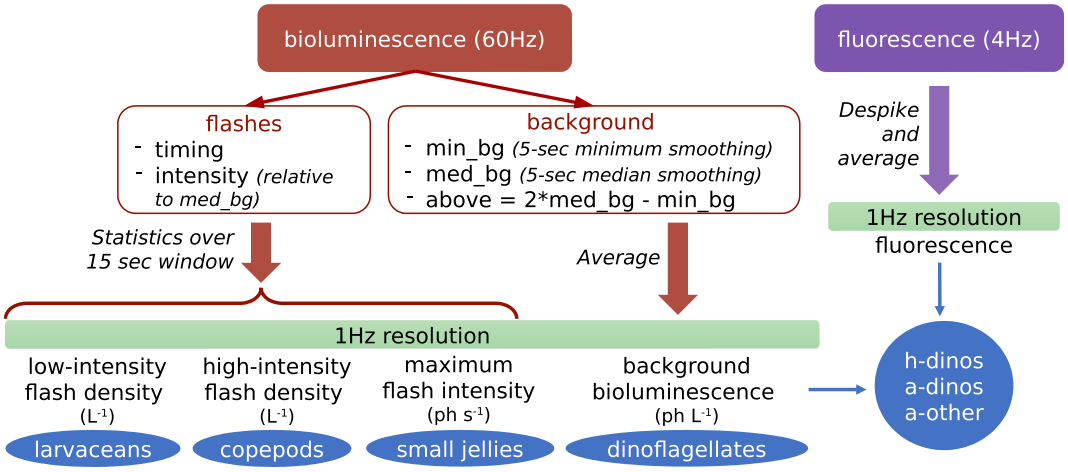

Fig. B1. Proxy processing workflow. The 60 Hz bioluminescence time series are processed to extract flashes and background. The bioluminescence proxies are then calculated at a lower resolution (1 Hz) by averaging the background at each time step and computing flash statistics over a longer time window (15 sec sliding window for AUVs). The background bioluminescence is then combined with fluorescence to separate the dinoflagellates into autotrophic and heterotrophic populations, and compute an additional proxy for non-dinoflagellate phytoplankton such as diatoms.

series. The median background (*med_bg*) is similarly obtained using a median function. The mean dinoflagellate bioluminescence is better represented by the median than mean bioluminescence, as the mean would be strongly contaminated by high values (zooplankton flashes i.e. non-dinoflagellate). It is assumed that dinoflagellate bioluminescence oscillates symmetrically around its mean, based on observations for high-concentration dinoflagellate populations (Latz and Rohr, 2013, their Fig. 2). The envelope is thus defined by using *min_bg* as the bottom limit, and defining the top limit symmetrically around *med_bg* (equal to 2 × *med_bg* - *min_bg*). Flashes are identified using the Matlab function peakfinder.m (https://mathworks.com/matlabcentral/fileexchange/25500-peakfinder); only flashes above the envelope are considered. The number of flashes per second is computed from the time series, and divided by the BP flow rate to obtain the number of flashes per liter. The proxies were computed within a 30 s (MUSE-2000 and SPOKES-2002) or 1 min (AOSN-2003) time window centered at the sample depth. The time window is longer for AOSN-2003 because the Schindler trap was maintained at the sample depth for longer.

Proxy parameters were optimized through sensitivity tests based on correlations with *in situ* counts, where a range of values is attributed to a parameter while holding the others constant. The parameter resulting in the highest correlation with *in situ* counts was chosen. An example is provided for the low/high flash intensity threshold in Fig. B2. These parameters are: the sliding window used to define the background (5 s for 60 Hz resolution, 10 s for 1 Hz), the 1 Hz flash threshold (2×10^{10} ph s^{-1} for MUSE-2000 and SPOKES-2002, 7.6×10^{9} ph s^{-1} for AOSN-2003), the 60 Hz minimum envelope (1.5×10^{10} ph s^{-1}) and the 60 Hz low/high flash intensity threshold (10^{11} ph s^{-1}). The reason for the lower 1 Hz flash threshold for AOSN-2003 is that a newer BP was used (Gen3, 60 Hz original resolution). The older BP (Gen2, 1 Hz only) was deployed alongside Gen3 for 17% of the profiles which enabled a comparison of two. The median Gen2/Gen3 (equal to 2.63) was used to adjust the flash threshold. Gen1 (used during MUSE-2000) was similar to Gen2, and Gen3 is functionally the same as the commercially available UBAT (http://www.seabird.com/ubat).

(2) *H-dino*, *a-dino* and *a-other* proxies

Background bioluminescence and fluorescence are used to calculate *h-dinos*, *a-dinos* and *a-other* proxies as a function of *ratioAdinos*. "Dinoflagellate fluorescence-equivalent" is calculated as *bgBL_fluo* = *bg_BL/ratioAdinos*; *bgBL_fluo* does not correspond to a measured fluorescence but to background bioluminescence expressed in fluorescence units, based on the *ratioAdinos* conversion. Proxies (in fluorescence units) are then defined as (Fig. 4b):

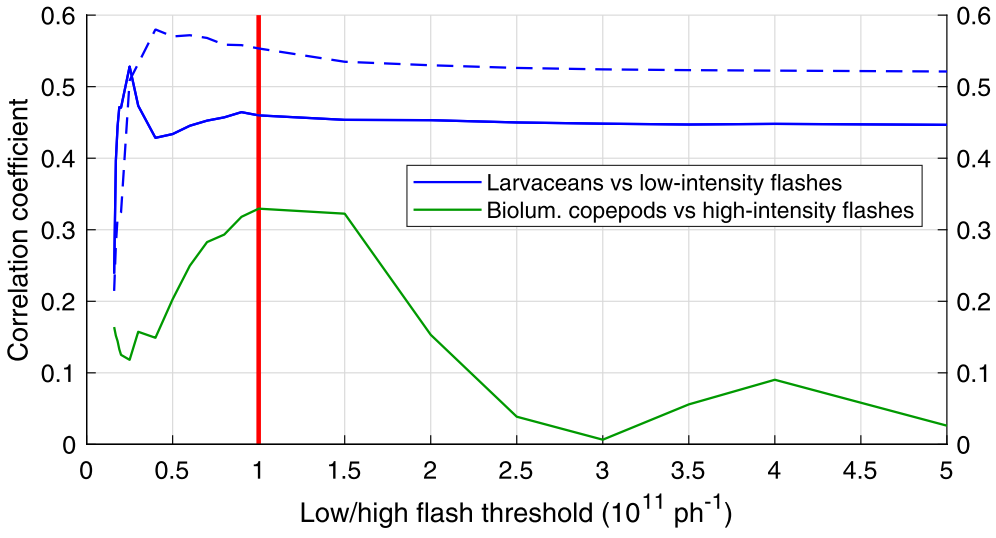

Fig. B2. Using sensitivity analysis to determine the flash threshold separating low- and high-intensity flashes (proxies for larvaceans and copepods). Correlations between concentrations and the proxies are displayed as a function of the flash threshold; the dashed line represents larvacean correlations restricted to samples with larvacean concentrations < 3.5 L^{-1} (better representative of larvacean flashes, see Section 3.1). The red bar highlights the resulting threshold (10^{11} ph s^{-1}), chosen as a compromise between both proxies (highest copepod correlation and still high larvacean correlation).

$a{-}dino = \min(fluo, bgBL\_fluo)$
$a{-}other = fluo{-}adino$
$h{-}dino = bgBL\_fluo{-}adino$

By definition, *a-other* = 0 when $fluo \leq bgBL\_fluo$, *h-dino* = 0 when $bgBL\_fluo \leq fluo$ so that for any (*fluo,bg BL*) combination, one of the 3 proxies is equal to 0. This means that 2 proxies are computed from 2 variables; which proxies these are (*a-dinos* and *a-other*, or *a-dinos* and *h-dinos*) depends on whether the (*fluo,bg BL*) point is located above or below the *ratioAdinos* line. The sum of the 3 proxies is equal to *fluo* if below the *ratioAdinos* line, *bgBL_fluo* if above.

Appendix C. Supplementary data

Supplementary data to this article can be found online at https://doi.org/10.1016/j.pocean.2018.12.010.

References

Batchelder, H.P., Swift, E., 1989. Estimated near-surface mesoplanktonic bioluminescence in the western North Atlantic during July 1986. Limnol. Oceanogr. 34, 113–128. https://doi.org/10.4319/lo.1989.34.1.0113.

Batchelder, H.P., Swift, E., Keuren, J.R.V., 1992. Diel patterns of planktonic bioluminescence in the northern Sargasso Sea. Mar. Biol. 113, 329–339. https://doi.org/10.1007/bf00347288.

Boss, E., Behrenfeld, M., 2010. In situ evaluation of the initiation of the North Atlantic phytoplankton bloom. Geophys. Res. Lett. 37, L18603. https://doi.org/10.1029/2010GL044174.

Buskey, E.J., 1992. Epipelagic planktonic bioluminescence in the marginal ice zone of the Greenland Sea. Mar. Biol. 113, 689–698. https://doi.org/10.1007/BF00349712.

Buskey, E.J., Swift, E., 1990. An encounter model to predict natural planktonic bioluminescence. Limnol. Oceanogr. 35, 1469–1485. https://doi.org/10.4319/lo.1990.35.7.1469.

Cetinić, I., Perry, M.J., D'Asaro, E., Briggs, N., Poulton, N., Sieracki, M.E., Lee, C.M., 2015. A simple optical index shows spatial and temporal heterogeneity in phytoplankton community composition during the 2008 North Atlantic Bloom Experiment. Biogeosciences 12, 2179–2194. https://doi.org/10.5194/bg-12-2179-2015.

Chavez, F.P., Pennington, J.T., Michisaki, R.P., Blum, M., Chavez, G.M., Friederich, J., Jones, B., Herlien, R., Kieft, B., Hobson, R., Ren, A.S., Ryan, J., Sevadjian, J.C., Wahl, C., Walz, K.R., Yamahara, K., Friederich, G.E., Messié, M., 2017. Climate variability and change: response of a coastal ocean ecosystem. Oceanography 30 (4), 128–145. https://doi.org/10.5670/oceanog.2017.429.

Craig, J., I. G. Priede (2012), Bioluminescence – a source of marine energy?, The Crown Estate.

Cronin, H.A., Cohen, J.H., Berge, J., Johnsen, G., Moline, M.A., 2016. Bioluminescence as an ecological factor during high Arctic polar night. Sci. Rep. 6, 36374. https://doi.org/10.1038/srep36374.

Dickey, T.D., 1988. Recent advances and future directions in multi-disciplinary in situ oceanographic measurement systems. In: Toward a theory on biological-physical interactions in the world ocean. Springer, Dordrecht, pp. 555–598.

Esaias, W.E., Curl, H.C., Seliger, H.H., 1973. Action spectrum for a low intensity, rapid photoinhibition of mechanically stimulable bioluminescence in the marine dinoflagellates Gonyaulax catenella, G. acatenella, and G. tamarensis. J. Cell. Physiol. 82, 363–372. https://doi.org/10.1002/jcp.1040820306.

Galt, C.P., Grober, M.S., 1985. Total stimulable luminescence of Oikopleura houses (Urochordata, Larvacea). Bull. Mar. Sci. 765.

Galt, C.P., Grober, M.S., Sykes, P.F., 1985. Taxonomic correlates of bioluminescence among appendicularians (Urochordata: Larvacea). Biol. Bulletin 168, 125–134.

Galt, C.P., Sykes, P.F., 1983. Sites of bioluminescence in the appendicularians Oikopleura dioica and O. labradoriensis (Urochordata: Larvacea). Mar. Biol. 77, 155–159. https://doi.org/10.1007/BF00396313.

Haddock, S.H.D., Moline, M.A., Case, J.F., 2010. Bioluminescence in the sea. Ann. Rev. Marine Sci. 2, 443–493. https://doi.org/10.1146/annurev-marine-120308-081028.

Harvey, J.B., Johnson, S.B., Fisher, J.L., Peterson, W.T., Vrijenhoek, R.C., 2017. Comparison of morphological and next generation DNA sequencing methods for assessing zooplankton assemblages. J. Exp. Mar. Biol. Ecol. 487, 113–126. https://doi.org/10.1016/j.jembe.2016.12.002.

Herren, C.M., Haddock, S.H.D., Johnson, C., Orrico, C.M., Moline, M.A., Case, J.F., 2005. A multi-platform bathyphotometer for fine-scale, coastal bioluminescence research. Limnol. Oceanogr. Methods 3, 247–262. https://doi.org/10.4319/lom.2005.3.247.

Herring, P.J., 1988. Copepod luminescence. Hydrobiologia 167–168, 183–195. https://doi.org/10.1007/BF00026304.

Herring, P.J., Latz, M.I., Bannister, N.J., Widder, E.A., 1993. Bioluminescence of the Poecilostomatoid copepod Oncaea-conifera. Mar. Ecol. Prog. Ser. 94, 297–309. https://doi.org/10.3354/meps094297.

Johnsen, G., Candeloro, M., Berge, J., Moline, M., 2014. Glowing in the dark: discriminating patterns of bioluminescence from different taxa during the Arctic polar night. Polar Biol. 37, 707–713. https://doi.org/10.1007/s00300-014-1471-4.

Kim, G., Lee, Y.-W., Joung, D.-J., Kim, K.-R., Kim, K., 2006. Real-time monitoring of nutrient concentrations and red-tide outbreaks in the southern sea of Korea. Geophys. Res. Lett. 33. https://doi.org/10.1029/2005GL025431.

Lapota, D., 1998. Long-term and seasonal changes in dinoflagellate bioluminescence in the Southern California Bight. University of California, Santa Barbara.

Lapota, D., 2012a. Long term dinoflagellate bioluminescence, chlorophyll, and their environmental correlates in Southern California coastal waters. In: Lapota, D. (Ed.), Bioluminescence - Recent Advances in Oceanic Measurements and Laboratory Applications. Intech doi:10.5772/35154.

Lapota, D., 2012b. Seasonal changes of bioluminescence in photosynthetic and heterotrophic dinoflagellates at San Clemente Island. In: Lapota, D. (Ed.), Bioluminescence - Recent Advances in Oceanic Measurements and Laboratory Applications. Intech doi:10.5772/35341.

Lapota, D., Galt, C., Losee, J.R., Huddell, H.D., Orzech, J.K., Nealson, K.H., 1988. Observations and measurements of planktonic bioluminescence in and around a milky sea. J. Exp. Mar. Biol. Ecol. 119, 55–81. https://doi.org/10.1016/0022-0981(88)90152-9.

Lapota, D., Geiger, M.L., Stiffey, A.V., Rosenberger, D.E., Young, D.K., 1989. Correlations of planktonic bioluminescence with other oceanographic parameters from a Norwegian fjord. Mar. Ecol. Prog. Ser. 55, 217–227.

Lapota, D., Losee, J.R., 1984. Observations of bioluminescence in marine plankton from the Sea of Cortez. J. Exp. Mar. Biol. Ecol. 77, 209–239.

Latz, M., Jeong, H., 1996. Effect of red tide dinoflagellate diet and cannibalism on the bioluminescence of the heterotrophic dinoflagellates Protoperidinium spp. Mar. Ecol. Prog. Ser. 132, 275–285. https://doi.org/10.3354/meps132275.

Latz, M.I., Nauen, J.C., Rohr, J., 2004. Bioluminescence response of four species of dinoflagellates to fully developed pipe flow. J. Plankton Res. 26, 1529–1546. https://doi.org/10.1093/plankt/fbh141.

Latz, M.I., Rohr, J., 2013. Bathyphotometer bioluminescence potential measurements: A framework for characterizing flow agitators and predicting flow-stimulated bioluminescence intensity. Cont. Shelf Res. 61–62, 71–84. https://doi.org/10.1016/j.csr.2013.04.033.

Lopez, P., O'Reilly, T.C., Klimov, D., 2015. Cytometers set sail with sea-going mobile robots. Mar. Technol. Soc. J. 49, 17–26. https://doi.org/10.4031/MTSJ.49.3.9.

Lorenzen, 1966. A method for the continuous measurement of in vivo chlorophyll concentration. Deep Sea Res. Oceanogr. Abstr. 13 (2), 223–227. https://doi.org/10.1016/0011-7471(66)91102-8.

Mahadevan, A., D'Asaro, E., Lee, C., Perry, M.J., 2012. Eddy-driven stratification initiates North Atlantic spring phytoplankton blooms. Science 337, 54–58. https://doi.org/10.1126/science.1218740.

Marcinko, C.L.J., Allen, J.T., Poulton, A.J., Painter, S.C., Martin, A.P., 2013a. Diurnal variations of dinoflagellate bioluminescence within the open-ocean north-east Atlantic. J. Plankton Res. 35, 177–190. https://doi.org/10.1093/plankt/fbs081.

Marcinko, C.L.J., Painter, S.C., Martin, A.P., Allen, J.T., 2013b. A review of the measurement and modelling of dinoflagellate bioluminescence. Prog. Oceanogr. 109, 117–129. https://doi.org/10.1016/j.pocean.2012.10.008.

Margalef, R., 1978. Life-forms of phytoplankton as survival alternatives in an unstable environment. Oceanologica Acta 1, 493–509.

Martini, S., Haddock, S.H.D., 2017. Quantification of bioluminescence from the surface to the deep sea demonstrates its predominance as an ecological trait. Sci. Rep. 7, 45750. https://doi.org/10.1038/srep45750.

Messié, M., Chavez, F.P., 2017. Nutrient supply, surface currents, and plankton dynamics predict zooplankton hotspots in coastal upwelling systems. Geophys. Res. Lett. 44, 8979–8986. https://doi.org/10.1002/2017GL074322.

Moline, M.A., Benoit-Bird, K., O'Gorman, D., Robbins, I.C., 2015. Integration of scientific echo sounders with an adaptable autonomous vehicle to extend our understanding of animals from the surface to the bathypelagic. J. Atmos. Oceanic Technol. 32, 2173–2186. https://doi.org/10.1175/JTECH-D-15-0035.1.

Moline, M.A., Blackwell, S.M., Case, J.F., Haddock, S.H.D., Herren, C.M., Orrico, C.M., Terrill, E., 2009. Bioluminescence to reveal structure and interaction of coastal planktonic communities. Deep-Sea Res. Part II 56, 232–245. https://doi.org/10.1016/j.dsr2.2008.08.002.

Morin, J.G., 1983. Coastal bioluminescence: patterns and functions. Bull. Mar. Sci. 33, 787–817.

Powell, J.R., Ohman, M.D., 2012. Use of glider-class acoustic Doppler profilers for estimating zooplankton biomass. J. Plankton Res. 34, 563–568. https://doi.org/10.1093/plankt/fbs023.

Richardson, T.L., Lawrenz, E., Pinckney, J.L., Guajardo, R.C., Walker, E.A., Paerl, H.W., MacIntyre, H.L., 2010. Spectral fluorometric characterization of phytoplankton community composition using the Algae Online Analyser®. Water Res. 44 (8), 2461–2472. https://doi.org/10.1016/j.watres.2010.01.012.

Rudnick, D.L., 2016. Ocean research enabled by underwater gliders. Ann. Rev. Marine Sci. 8, 519–541. https://doi.org/10.1146/annurev-marine-122414-033913.

Santora, J.A., Sydeman, W.J., Messié, M., Chai, F., Chao, Y., Thompson, S.A., Wells, B.K.,

Chavez, F.P., 2013. Triple check: observations verify structural realism of an ocean ecosystem model. Geophys. Res. Lett. 40, 1367–1372. https://doi.org/10.1002/grl.50312.

Shulman, I., Moline, M.A., Penta, B., Anderson, S., Oliver, M., Haddock, S.H.D., 2011. Observed and modeled bio-optical, bioluminescent, and physical properties during a coastal upwelling event in Monterey Bay, California. J. Geophys. Res.: Oceans 116, C01018. https://doi.org/10.1029/2010JC006525.

Shulman, I., Penta, B., Moline, M.A., Haddock, S.H.D., Anderson, S., Oliver, M.J., Sakalaukus, P., 2012. Can vertical migrations of dinoflagellates explain observed bioluminescence patterns during an upwelling event in Monterey Bay, California? J. Geophys. Res. Oceans 117, C01016. https://doi.org/10.1029/2011JC007480.

Shulman, I., Penta, B., Richman, J., Jacobs, G., Anderson, S., Sakalaukus, P., 2015. Impact of submesoscale processes on dynamics of phytoplankton filaments. J. Geophys. Res. Oceans 120 (3), 2050–2062. https://doi.org/10.1002/2014JC010326.

Smayda, T.J., Trainer, V.L., 2010. Dinoflagellate blooms in upwelling systems: seeding, variability, and contrasts with diatom bloom behaviour. Prog. Oceanogr. 85, 92–107. https://doi.org/10.1016/j.pocean.2010.02.006.

Swift, E., Sullivan, J.M., Batchelder, H.P., Van Keuren, J., Vaillancourt, R.D., Bidigare, R.R., 1995. Bioluminescent organisms and bioluminescence measurements in the North Atlantic Ocean near latitude 59.5 N, longitude 21 W. J. Geophys. Res. Oceans 100, 6527–6547. https://doi.org/10.1029/94JC01870.

Trainer, V.L., Pitcher, G., Reguera, B., Smayda, T., 2010. The distribution and impacts of harmful algal bloom species in eastern boundary upwelling systems. Prog. Oceanogr. 85, 33–52. https://doi.org/10.1016/j.pocean.2010.02.003.

Valiadi, M., Iglesias-Rodriguez, D., 2013. Understanding bioluminescence in dinoflagellates - how far have we come? Microorganisms 1, 3–25. https://doi.org/10.3390/microorganisms1010003.

Wong, C.K., 1988. The swimming behavior of the copepod Metridia pacifica. J. Plankton Res. 10 (6), 1285–1290. https://doi.org/10.1093/plankt/10.6.1285.